

ISTANBUL TECHNICAL UNIVERSITY
FACULTY OF ELECTRICAL AND ELECTRONICS ENGINEERING

AUTONOMOUS LANDING OF NASA-GTM AIRCRAFT

CONTROL AND AUTOMATION ENGINEERING DESIGN II

**Furkan ÇİFTLİKÇİ
Ebubekir DENİZHAN
Agah Enes SOYALP**

Control and Automation Engineering

Thesis Advisor: Assoc. Prof. İlker ÜSTOĞLU

01/2024

ISTANBUL TECHNICAL UNIVERSITY
FACULTY OF ELECTRICAL AND ELECTRONICS ENGINEERING

AUTONOMOUS LANDING OF NASA-GTM AIRCRAFT

CONTROL AND AUTOMATION ENGINEERING DESIGN II

Furkan ÇİFTLİKÇİ (040210771)
Ebubekir DENİZHAN (040180618)
Agah Enes SOYALP (040190616)

Kontrol ve Otomasyon Mühendisliği

Control and Automation Engineering

01/2024

To all the babies who are killed in Gaza...

FOREWORD

First and foremost, we extend our gratitude to our thesis advisor, Assoc. Prof. İlker ÜSTOĞLU, and to Talha ULUKIR, who assisted us in preparing this thesis.

We would like to express our appreciation to our beloved family members, university professors who have always been by our side throughout our university journey, and all our friends who have contributed to making our university experience enjoyable.

As aspiring control engineers, we aim to work diligently and become experts in our field, and we will strive to do our best in pursuit of this goal.

01/2024

Furkan ÇİFTLİKÇİ
Ebubekir DENİZHAN
Agah Enes SOYALP

TABLE OF CONTENTS

	<u>Page</u>
FOREWORD.....	v
TABLE OF CONTENTS.....	vii
ABBREVIATIONS	ix
SYMBOLS	xi
LIST OF TABLES	xiii
LIST OF FIGURES	xv
ÖZET.....	xviii
SUMMARY	xx
1 INTRODUCTION.....	2
1.1 Purpose of Thesis	2
1.2 Literature Review	3
1.3 Motivation.....	4
2 MODELLING OF GTM AIRCRAFT	5
2.1 Mathematical Modelling	8
2.1.1 Reference Frames.....	8
2.1.1.1 Inertial Frame	9
2.1.1.2 Earth-Centered Earth-Fixed Frame	9
2.1.1.3 Vehicle Carried Frame	10
2.1.1.4 Wind-Fixed Frame	10
2.1.1.5 Stability Frame.....	10
2.1.1.6 Body-Fixed Frame	11
2.1.2 Frame Rotation.....	12
2.1.3 Forces and Moments	12
2.1.4 Angles, Angular Velocity and Rates.....	13
2.1.5 6-DOF Equations of Motions.....	14
2.1.5.1 3-DoF Translational Equations	15
2.1.5.2 3-DoF Rotational Equations.....	15
2.1.6 Translational Kinematics	17
2.1.7 Rotational Kinematics.....	17
2.2 Trim and Linearization.....	18
2.2.1 Trim Definition and Purpose.....	18
2.2.2 Linearization	18
2.2.3 Trim Conditions	19
2.3 Aircraft Modes	22
2.3.1 Longitudinal Modes	22
2.3.1.1 Phugoid mode	23
2.3.1.2 Short-period mode.....	23
2.3.2 Lateral-directional Modes	24
2.3.2.1 Roll mode	24
2.3.2.2 Dutch-roll mode	25
2.3.2.3 Spiral mode	26
3 LANDING PHASES	27
3.1 Base Leg.....	27
3.2 Glide	27
3.3 Flare.....	27
3.4 Touchdown.....	28

3.5 Taxi.....	28
4 OPEN-LOOP ANALYSIS.....	29
4.1 Transfer Functions.....	31
4.1.1 Transfer Functions of Elevator.....	31
4.1.2 Transfer Functions of Aileron	33
4.1.3 Transfer Functions of Rudder	34
5 FLIGHT CONTROLLER DESIGN.....	35
5.1 Longitudinal Controller	35
5.1.1 Stability Augmentation, Pitch Damper (q-SAS).....	36
5.1.2 Inner Loop, Pitch Attitude Hold.....	36
5.1.3 Outer Loop, Altitude Hold	38
5.1.4 True Airspeed (TAS) Control	39
5.2 Lateral Controller	41
5.2.1 Stability Augmentation, Roll Damper (p-SAS)	42
5.2.2 Inner Loop, Wing Leveler	42
5.2.3 Outer Loop, Heading Angle Hold.....	44
5.2.4 Sideslip Angle Control.....	46
6 SIMULATION AND RESULTS.....	49
6.1 Base Leg	49
6.1.1 Heading Angle Arrangement	50
6.1.2 Speed Adjustment	51
6.1.3 Flaps Extension	52
6.2 Glide Phase.....	53
6.3 Flare Phase.....	55
6.4 Touchdown	57
REFERENCES	58
APPENDIX	60

ABBREVIATIONS

AOA	Angle of Attack
DOF	Degree of Freedom
EAS	Equivalent Airspeed
ECEF	Earth Centered and Earth Fixed
FCS	Flight Control System
GTM	Generic Transportation Model
IAS	Indicated Airspeed
NASA	National Aeronautics and Space Administration
PI	Proportional Integral
PID	Proportional Integral Derivative
SAS	Stability Augmentation System
SSA	Sideslip Angle
TAS	True Airspeed

SYMBOLS

x_w	: Longitudinal axis of Wind Fixed Reference Frame
y_w	: Lateral axis of Wind Fixed Reference Frame
z_w	: Vertical axis of Wind Fixed Reference Frame
x_E	: Longitudinal axis of Inertial Reference Frame
y_E	: Lateral axis of Inertial Reference Frame
z_E	: Vertical axis of Inertial Reference Frame
x_{ECEF}	: Longitudinal axis of ECEF Reference Frame
y_{ECEF}	: Lateral axis of ECEF Reference Frame
z_{ECEF}	: Vertical axis of ECEF Reference Frame
x_v	: Longitudinal axis of Vehicle Carried Reference Frame
y_v	: Lateral axis of Vehicle Carried Reference Frame
z_v	: Vertical axis of Vehicle Carried Reference Frame
x_s	: Longitudinal axis of Stability Reference Frame
y_s	: Lateral axis of Stability Reference Frame
z_s	: Vertical axis of Stability Reference Frame
x	: Longitudinal axis of Body Fixed Reference Frame
y	: Lateral axis of Body Fixed Reference Frame
z	: Vertical axis of Body Fixed Reference Frame
C	: Origin of Body Fixed Reference Frame
p	: Roll Rate
q	: Pitch Rate
r	: Yaw Rate
u	: Velocity Component in Longitudinal axis for F_B
v	: Velocity Component in Lateral axis for F_B
w	: Velocity Component in Vertical axis for F_B
L	: Rolling Moment
M	: Pitching Moment
N	: Yawing Moment
X	: Longitudinal Force
Y	: Lateral Force
Z	: Vertical Force
F_w	: Wind Fixed Reference Frame
F_B	: Body Fixed Reference Frame
α	: AOA
β	: SSA
θ	: Pitch or Slope Angle
ϕ	: Bank or Roll Angle
ψ	: Head or Azimuth Angle
I	: Inertia Matrix
T	: Transformation Matrix
ζ	: Damping Ratio
w_n	: National Frequency
γ	: Flight Path Angle
τ	: Time Constant
V_{stall}	: Stall Speed

LIST OF TABLES

	<u>Page</u>
Table 1. Notation names of body-fixed frame	12
Table 2. Phugoid mode properties	23
Table 3. Short-period mode properties.....	24
Table 4. Roll mode properties	25
Table 5. Dutch-roll mode properties	26
Table 6. Spiral mode properties	26
Table 7. Trim point	29
Table 8. Control surface limits.....	35
Table 9. Pitch attitude hold controller gains	38
Table 10. Altitude hold controller gains	39
Table 11. TAS controller gains	41
Table 12. Wing leveler controller gains	44
Table 13. Heading angle controller gains	46
Table 14. Sideslip angle controller gains	48
Table 15. Stall speeds according to flaps position	56

LIST OF FIGURES

	<u>Page</u>
Figure 1. Accidents by phase of flight	3
Figure 2. All aircrafts developed for the pilot training program.....	5
Figure 3. GTM T2 aircraft model on SIMULINK	6
Figure 4. Some blocks of the GTM-T2 plant.....	6
Figure 5. Actuators block	7
Figure 6. Actuator dynamics block	7
Figure 7. Equation of motion block	8
Figure 8. Gravity model block	8
Figure 9. Inertial reference frame.....	9
Figure 10. ECEF reference frame	10
Figure 11. Notation of body-fixed frame	11
Figure 12. Forces effecting the aircraft	13
Figure 13. Euler angles	14
Figure 14. Phugoid mode effect on aircraft	23
Figure 15. Short-period mode effect on aircraft.....	23
Figure 16. Roll mode effect on aircraft.....	24
Figure 17. Dutch-roll mode effect on aircraft	25
Figure 18. Spiral mode effect on aircraft	26
Figure 19. Landing phases	27
Figure 20. Flare maneuver for soft and safe touchdown.....	28
Figure 21. Angular velocities and rates according to control surfaces doublets.....	30
Figure 22. Linear velocities according to control surfaces doublets.....	31
Figure 23. Pole-Zero Map of $\partial\theta\partial\text{Elevator}$	32
Figure 24. Pole-Zero Map of $\partial q\partial\text{Elevator}$	32
Figure 25. Pole-Zero Map of $\partial\phi\partial\text{Aileron}$	33
Figure 26. Pole-Zero Map of $\partial p\partial\text{Aileron}$	33
Figure 27. Pole-Zero Map of $\partial\beta\partial\text{Rudder}$	34
Figure 28. Pole-Zero Map of $\partial r\partial\text{Rudder}$	34
Figure 29. Pitch attitude hold controller block diagram	37
Figure 30. Pitch attitude hold controller design	37
Figure 31. Altitude hold controller block diagram	38
Figure 32. Altitude hold controller design	39
Figure 33. Velocity controller block diagram	40
Figure 34. Velocity controller design.....	40
Figure 35. Wing leveler controller block diagram	43
Figure 36. Wing leveler controller design.....	43
Figure 37. Heading angle controller block diagram.....	44
Figure 38. Heading angle controller design	45
Figure 39. Direct and filtered signal comparison.....	45
Figure 40. Heading angle alignment	46
Figure 41. Sideslip - β angle representation.....	47
Figure 42. Sideslip angle controller design.....	47
Figure 43. Boeing 777-300 in FlightGear simulator	49
Figure 44. Altitude, TAS and heading angle graphics	49
Figure 45. Altitude and TAS graphics during roll maneuver.....	50

Figure 46. Lateral controller graphics during roll maneuver	50
Figure 47. Sideslip angle controller graphic during roll maneuver.....	51
Figure 48. Velocity controller graphics during speed adjustment	51
Figure 49. Longitudinal controller graphics during speed adjustment.....	52
Figure 50. Velocity controller graphics during flaps extension	53
Figure 51. Longitudinal controller graphics during flaps extension	53
Figure 52. Longitudinal controller graphics at glide phase.....	54
Figure 53. Velocity controller graphics at glide phase.....	54
Figure 54. Vertical speed and gamma angle graphics at glide phase.....	55
Figure 55. Desired exponential flare path	55
Figure 56. Longitudinal controller graphics at flare	56
Figure 57. Velocity behavior at flare	56
Figure 58. Vertical speed and gamma angle graphics at flare	57

NASA-GTM UÇAĞININ OTONOM İNİŞİ

ÖZET

Bu tez çalışması, çift motorlu bir yolcu uçağı için otomatik iniş sistemi tasarlanmasıyla ilgili kritik bir aşama olan iniş sürecini ele almaktadır. Tez, otomatik iniş otopilotu için literatürde bulunan iniş fazlarını ve kontrol mimarilerini inceleyerek başlamaktadır. Hava aracının modellemesinde, havacılıkta kullanılan eksen takımları, dönüşüm, kuvvet ve moment denklemleri, eyleyici ve sensör modelleri ele alınmıştır.

Hava aracı kontrol sistemleri genellikle doğrusal olmayan modeller üzerine kurulabilir, ancak literatürde çeşitli koşullarda doğrusal model elde etme ve bu model üzerinden kontrol mimarisini oluşturma yaklaşımları bulunmaktadır. Bu nedenle, tez içinde denge noktasını bulma ve bu nokta etrafında doğrusallaştırma konularına da değinilmektedir. Farklı koşullarda doğrusallaştırma sonuçları incelenmiş ve sistem giriş-çıkış değişiklikleri üzerindeki etkiler analiz edilmiştir.

Otomatik iniş otopilotu tasarımda uluslararası standartlar ve kabuller mevcuttur. Bu standartlar, güvenli inişi alt fazlara böler ve bu fazlar tüm sistemlerde benzer şekilde yer alır. Tez, otomatik iniş otopilotuna ait alt fazları ve bu fazların kriterlerini ve koşullarını incelemektedir. Havacılıkta kullanılan uçuş kontrol sistemlerinin incelenmesi, pilot otoritesi olan kontrol mimarilerinden başlayarak tam otonom mimarilere kadar uzanmaktadır. Sabit kanatlı hava aracı kontrol sistemlerinde, boyolamsal ve yanal durumlar ayrılarak incelenir. Uçuş kontrolünde boyolamsal ve yanal modların kutupları üzerinden sistem karakteristikleri ele alınmış ve tez kapsamındaki hava aracının modları detaylı bir şekilde incelenmiştir.

Farklı şartlarda gerçekleştirilen doğrusallaştırma sonuçlarına göre, sistem girişlerinin, sistem doğal frekanslarının ve sönüm oranlarının değişimi incelenmiştir. Tez kapsamında, iniş sistemi için tasarlanan kontrolcü PID kontrol mimarisine sahiptir. Bu kontrol mimarisini, tek giriş-tek çıkış kontrol yapısını benimsemektedir. PID kontrolörünün tasarlanma amacı, ulaşılabilir ve havacılıkta yaygın olarak kullanılan bir kontrol yapısı olmasıyla birlikte otomatik iniş problemindeki uygulanabilirliğini incelemektedir. Tez kapsamında tasarlanan iniş otopilotu, klasik iniş mimarilerinde olduğu gibi süzülme, palye ve teker koyma alt fazlarından oluşmaktadır. Iniş simülasyonu ve performans analizleri doğrusal olmayan model temel alınarak yapılmıştır. Tezin değerlendirme bölümünde, yanal ve boyolamsal kontrolcülerin belirli

kriterler altında, inişin tamamı boyunca başarıları değerlendirilerek, iniş otopilotu tasarımdaki başarı ele alınmıştır.

Anahtar Kelimeler: Otonom İniş, PID, Otopilot, İniş Aşamaları, Doğrusallaştırma, Trim Noktası

AUTONOMOUS LANDING OF NASA-GTM AIRCRAFT

SUMMARY

This thesis focuses on the crucial aspect of the landing process, specifically in the development of an automatic landing system for a twin-engine passenger aircraft. The descent phase involves a period of heightened disruptor activity, emphasizing the need to effectively respond to disruptions and ensure the system's resilience. The study commences by exploring diverse control architectures outlined in the literature for the automatic landing autopilot. The modeling of the aircraft encompasses discussions on axis sets, transformations, force and moment equations, as well as actuator and sensor models commonly used in aviation.

While aircraft control systems typically rest on nonlinear models, the literature presents approaches to derive a linear model under varied conditions and construct a control architecture based on this model. Consequently, the thesis delves into the issues of identifying equilibrium points and the linearization process around these points. The results of linearization are examined under different conditions, and the impact on changes in system input-output is thoroughly analyzed.

In the realm of automatic landing autopilot design, international standards and acceptances play a pivotal role. These standards categorize safe landings into subphases, consistently present across all systems. The thesis extensively investigates the subphases of the automatic landing autopilot, explaining the criteria and conditions associated with each phase. The exploration of flight control systems employed in aviation spans from control architectures with pilot authority to fully autonomous architectures. Within fixed-wing aircraft control systems, longitudinal and lateral situations are carefully examined. The study of flight control delves into system characteristics through the poles of longitudinal and lateral modes, offering a detailed examination of the aircraft modes within the thesis's scope.

In line with the linearization outcomes conducted under diverse circumstances, alterations in system inputs, system natural frequencies, and damping ratios are investigated. The landing system's controller, devised within the thesis, follows a PID control architecture, embracing a single-input, single-output control framework. The design objective of the PID controller is to assess its applicability to the automatic landing problem, given its accessibility and widespread use in aviation as a control

structure. The landing autopilot, formulated within the thesis, encompasses the subphases of gliding, flare, and wheel touchdown, like conventional landing architecture. Landing simulation and performance analyses are conducted based on the non-linear model. The thesis's evaluation segment deliberated on the success of the landing autopilot design by appraising the performance of lateral and longitudinal controller under predefined criteria throughout the entire landing process.

Keywords: Autoland, PID, Autopilot, Landing Phases, Linearization, Trim Point

1 INTRODUCTION

1.1 Purpose of Thesis

This thesis aims to design a PID (Proportional-Integral-Derivative) controller for the autonomous landing process of a fixed-wing NASA-GTM aircraft. The research will begin by obtaining the mathematical model of the aircraft, followed by the trimming and linearization of the acquired model to establish a foundation for PID controller design. The primary objectives of the thesis are outlined as follows:

- *Mathematical Modeling and Linearization:* Obtain the motion equations of the aircraft, bring these equations to equilibrium, and subsequently linearize them. This step forms the basis for the design of the PID controller.
- *Controller Design:* Utilizing the results of open-loop analysis, design a PID controller that operates effectively during the autonomous landing process. Adjust control parameters to meet the specified performance criteria.
- *Simulation and Performance Analysis:* Implement the developed PID controller in a simulation environment and subject it to various scenarios to test its performance. The analysis will focus on factors such as stability, precision, and speed during the landing process.
- *Results and Evaluation:* The thesis will summarize the obtained results and evaluate the performance of the PID controller design in the context of autonomous landing.

This thesis endeavors to present a practical approach to PID controller design in the realm of autonomous landing, providing insights into the advantages, limitations, and avenues for further enhancement of the proposed control system.

1.2 Literature Review

The history of aviation has witnessed significant advancements from the pioneering flight by the Wright brothers to the present day. These developments have amplified the challenges faced by pilots in maneuvering aircraft, consequently giving rise to the need for automatic flight control systems.

Automatic flight control systems find extensive applications in commercial, military, and general aviation. In general aviation, while aircraft are expected to operate in a free-flight environment, the majority still rely on manually operated control systems. The fundamental objective of automatic flight control systems is to alleviate the pilot's workload and enhance the safety of flight operations. [13]

It is possible to shortly list the stages of a flight as follows,

- Take-off
- Initial Climb
- Final Approach
- Landing

Among the most critical stages of a flight are takeoff, initial climb, final approach, and landing. The landing phase, as depicted in Figure 1, is observed to be the flight phase where aircraft accidents most frequently occur. Consequently, the automatic execution of the landing process can play a pivotal role in preventing aircraft accidents.

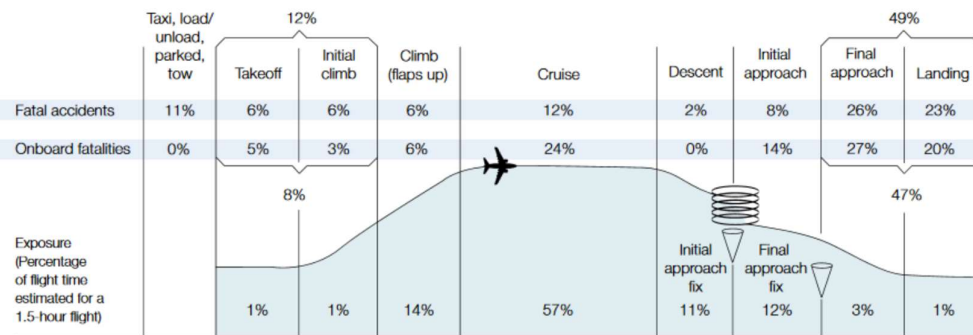


Figure 1. Accidents by phase of flight

In automatic landing algorithms, the most commonly used control structures are PID and its derivatives, as well as classical methods such as gain tuning and pole placement. [7]

Another automatic landing algorithm, featuring neural-assisted control architecture that enhances fault tolerance capabilities, is utilized for high-performance fighter aircraft facing issues like severe winds and control surface jamming. [17]

Fuzzy control methodology is another control approach used for automatic landing in both linear and nonlinear systems. [14]

The Robust control structure with H-infinity methodology is employed in automatic landing algorithms to reduce the adverse effects of disturbances and uncertainties during flight, enhancing resilience in challenging weather conditions. [16]

Another control approach for automatic landing involves the integration of dynamic inversion and adaptive control methods. The landing process is controlled through nested dual loops; the inner loop manages pitch angle, speed, and yaw rate, while the outer loop controls the landing slope. [12]

Additionally, by utilizing a sliding mode control structure in the design of the automatic landing controller, smooth execution of rapid alignment and flare maneuvers can be achieved through reference sliding. [18]

1.3 Motivation

The landing phase is known as one of the trickiest parts of flying, often associated with higher accident rates. Improving safety during this critical stage calls for the development of an autonomous landing system. To achieve this, we need to model and simplify different flight phases and then create a specialized controller.

In our early attempts, we used a PID controller to successfully manage the descent phase. In future projects, we plan to explore various types of controllers, comparing them thoroughly in a simulated environment. Our goal extends beyond simulations, we aim to validate promising results in real-world situations, bridging the gap between simulated and actual system performance.

Our ultimate aim is not just accident prevention during landings but creating a robust and adaptable autonomous landing system seamlessly integrated into real aviation operations. Through these efforts, we hope to contribute to improving aviation safety and efficiency.

2 MODELLING OF GTM AIRCRAFT

The chosen aircraft model for the thesis is the Generic Transport Model (GTM), which is also available in the NASA Technology Transfer Program. NASA's Aviation Safety Program conducted research using the T-2 tail-numbered aircraft as seen in Phase 3 in Figure 2, developed under the General Transport Model, to investigate situations arising from loss of control in aircraft. [9]

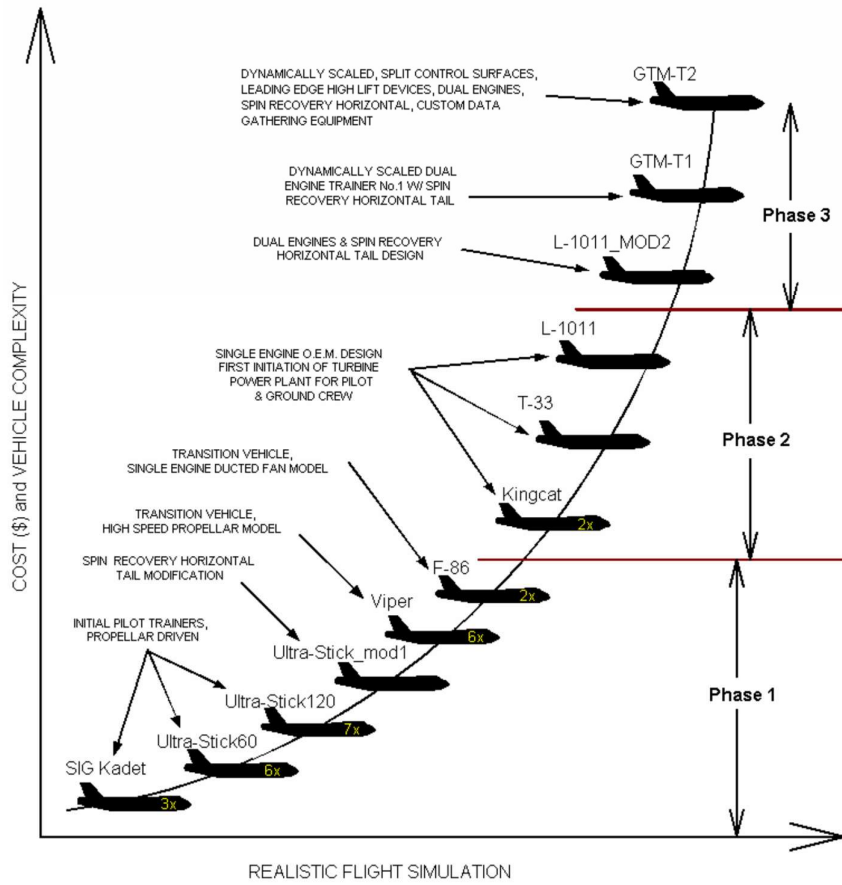


Figure 2. All aircraft developed for the pilot training program

Although designed as a geometrically 5.5% subscale version of a passenger plane, the aircraft is dynamically scaled. The goal is to advance flight control technologies capable of managing control during instances of damage or malfunction in this aircraft. The model incorporates not only the non-linear characteristics of the aircraft but also varying behaviors in error scenarios. Following classical aircraft modeling studies, flights were executed, resulting in the final model version. In this regard, dynamic scaling techniques were employed to appropriately scale flight dynamics. [1]

The computer model of the GTM_T2 aircraft was created in the SIMULINK environment. As seen in Figure 3, a structure to be controlled with aircraft model inputs has been established.

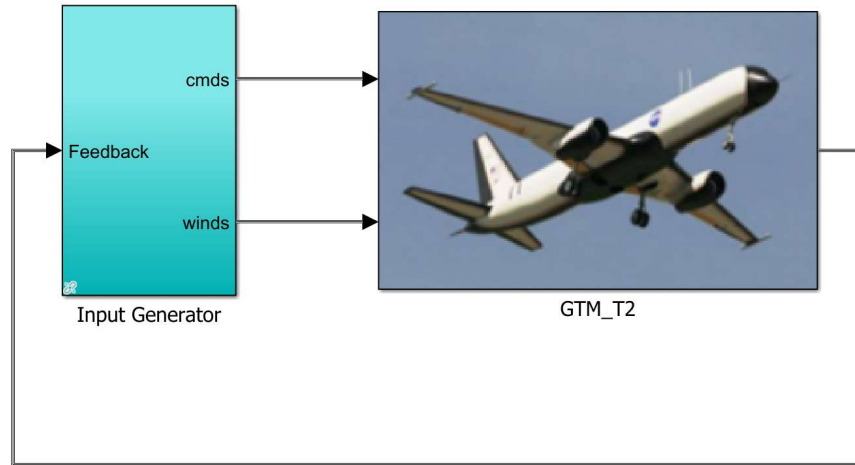


Figure 3. GTM T2 aircraft model on SIMULINK

To create the GTM_T2 plant, the actuator, engine, sensor, and dynamic features of the aircraft must be known. Equations of motion must also be created along with this. For the model part on SIMULINK, actuator, motors, sensors, gravity, aerodynamics, and equations of motion models were created in the form of blocks. Definitions have been made within these blocks. Blocks representations are given in Figure 4.

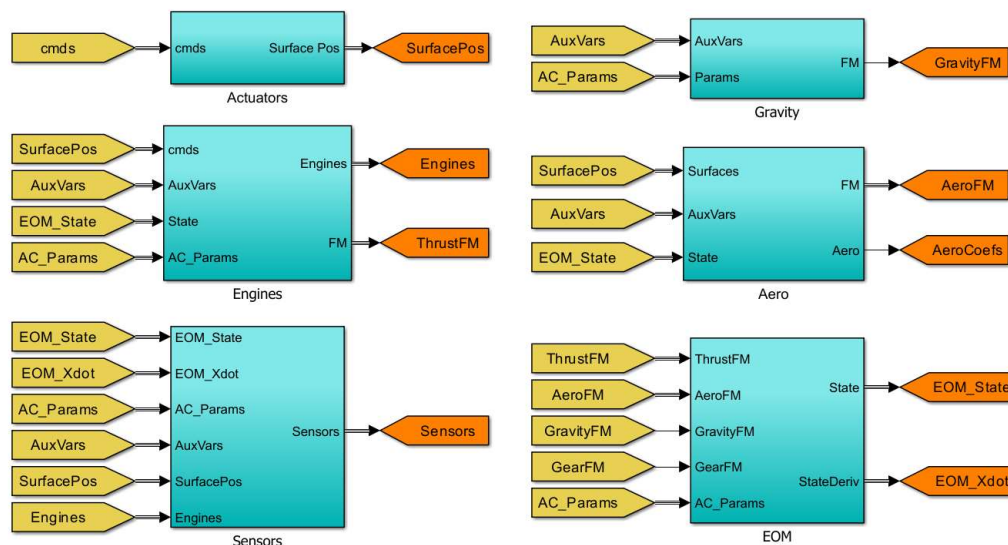


Figure 4. Some blocks of the GTM-T2 plant

A structure as in Figure 5 was established to model the actuator dynamics. Initially, dynamics were determined for each actuator. Time delays, surface bias and delta parameters are included in the model as values.

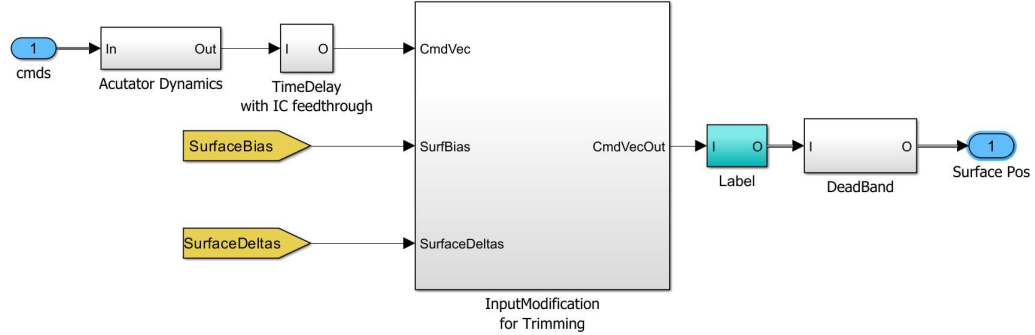


Figure 5. Actuators block

Aileron and Rudder Actuator dynamics are shown as examples in Figure 6. Special blocks were created by selecting appropriate parameters to model the dynamics of all actuators in the aircraft.

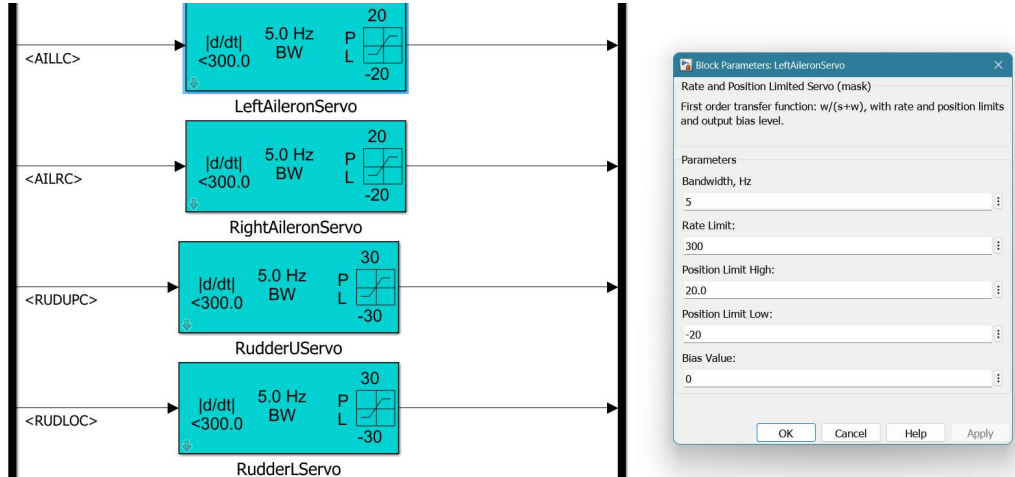


Figure 6. Actuator dynamics block

The equations of motion were modeled by designing a 6-DOF block. This block takes the equation parameters as input and shows the states of the system at the output. The system shown in Figure 7 has been established.

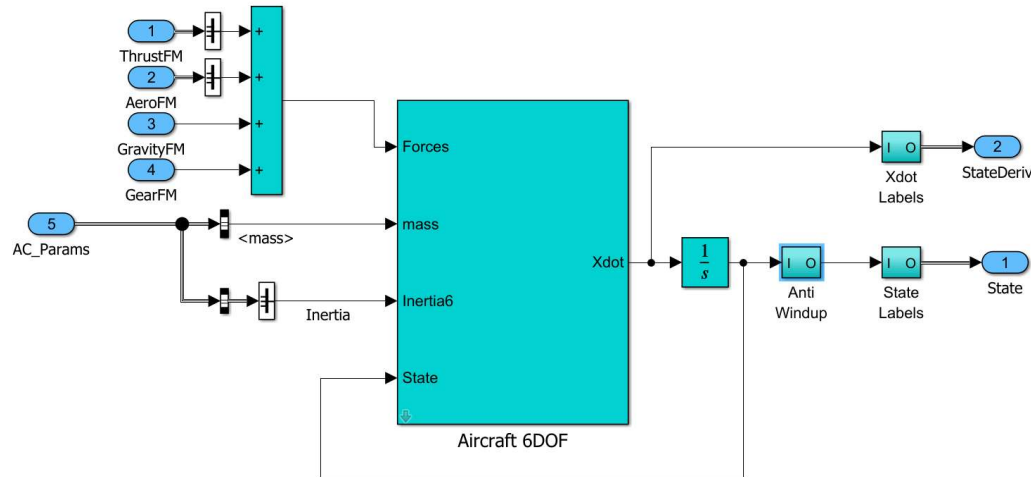


Figure 7. Equation of motion block

The gravity model can be seen in Figure 8.

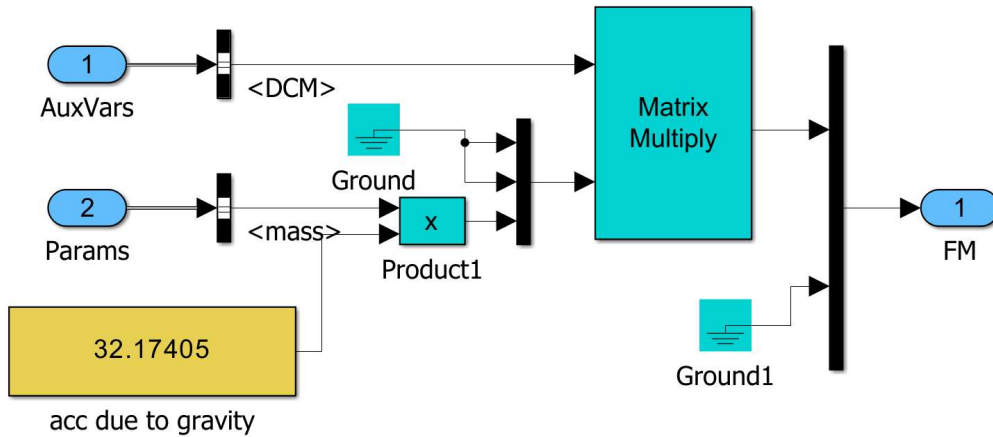


Figure 8. Gravity model block

For further information, please refer to APPENDIX section.

2.1 Mathematical Modelling

2.1.1 Reference Frames

To be able to describe the movements of aircraft and create appropriate mathematical models, appropriate axis sets must be determined and defined. Each axis set can offer different advantages depending on their intended use. The most used reference frames in aviation are explained in this thesis.

2.1.1.1 Inertial Frame

In each dynamics problem, the presence of an inertial reference frame is essential, whether explicitly stated or subtly implied. This frame remains either fixed or experiences uniform rectilinear translation concerning distant stars, [5]. Inertial Frame is associated with a situation in space or when an observer is on a non-accelerating object. If a reference frame is Inertial, meaning there is no net force acting on it, or the net force is zero, it is considered an Inertial Frame. The Earth's rotation axis and the equatorial plane can form the axes of the Inertial Frame.

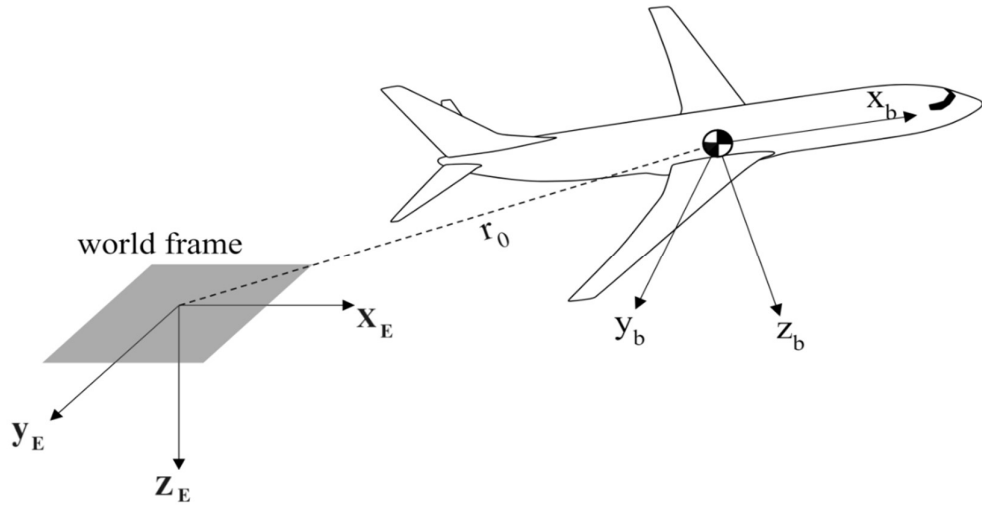


Figure 9. Inertial reference frame

2.1.1.2 Earth-Centered Earth-Fixed Frame

In Earth-Centered Earth-Fixed Frame (ECEF), the origin is fixed at the center of the Earth, providing a geocentric perspective. The x-axis points towards the intersection of the Prime Meridian and the Equator, the y-axis aligns with the Prime Meridian, and the z-axis completes the right-handed orthogonal system, directed towards the North Pole. Notably, the ECEF frame remains inertial, overcoming the challenges associated with the Earth's rotation by rotating along with the planet. This inertial characteristic simplifies the representation of global positions, velocities, and accelerations, making the ECEF frame a crucial tool in the accurate modeling, analysis, and navigation of aerospace systems.

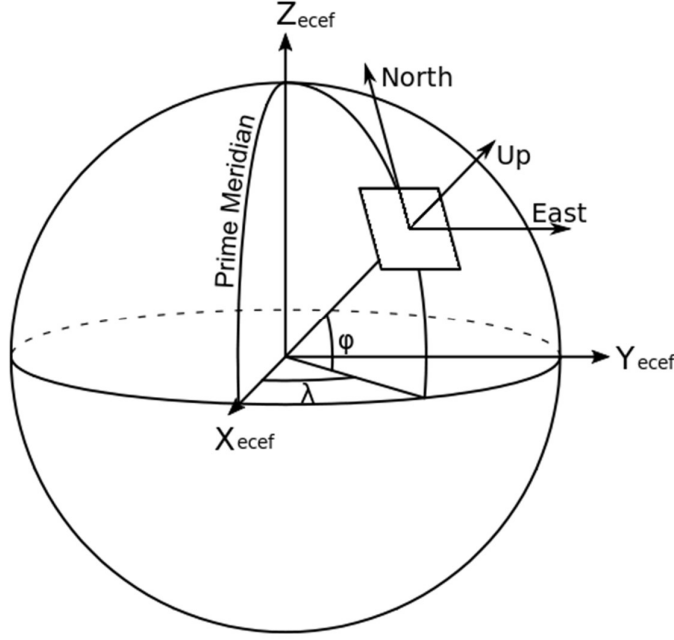


Figure 10. ECEF reference frame

2.1.1.3 Vehicle Carried Frame

Regardless of the orientation of the aircraft, axis orientations are made depending on Geographic North, Geographic East, and gravity vector. Although this frame is not related to the turns of the vehicle, it is attached to the vehicle. The X-axis (X_v) is defined towards the north of the Earth. Z-axis (Z_v) is pointing towards the local gravity vector. Y-axis (Y_v) points towards East.

2.1.1.4 Wind-Fixed Frame

Also known as Air trajectory reference frame, it refers to a coordinate system in which wind speed and direction are taken into consideration. When the wind moves relative to the aircraft or the aircraft interacts with the wind, this framework can be important. The X-axis (X_w) is defined towards the local air velocity vector. Z-axis (Z_w) is again pointing downwards in the plane of symmetry of the aircraft. Y-axis (Y_w) is determined according to the status of the Z_w and X_w axes.

2.1.1.5 Stability Frame

The stability framework, a unique configuration of body axes, are predominantly employed to examine minor perturbations from a stable reference flight state, [5]. It often plays an important role in the analysis of aerodynamics and flight control

systems. The stability of the aircraft is evaluated through various forces and moments within this frame. X-axis (X_s) is defined towards the relative wind vector. Z-axis (Z_s) is again pointing downwards in the plane of symmetry of the aircraft. Y-axis (Y_s) is determined according to the status of the Z_s and X_s axes.

2.1.1.6 Body-Fixed Frame

A body-fixed reference frame is defined as a set of axes affixed to a rigid body. Typically, the mass center C serves as the origin for these body axes. In the realm of flight dynamics, body axes hold particular significance, and there exists a convention of notation linked to them, [5]. Body Frame or Local Frame is attached to the body of the aircraft and moves and rotates with it. The x-axis is pointing towards the nose of the aircraft, while the z-axis is located on the axis of symmetry and is pointing downwards. The Y axis is determined according to the status of the Z and X axes. This axis set is used to show the forces acting on the aircraft and the structural conditions of the vehicle itself.

General notations linked to body-fixed frame are given in Figure 11 and Table 1.

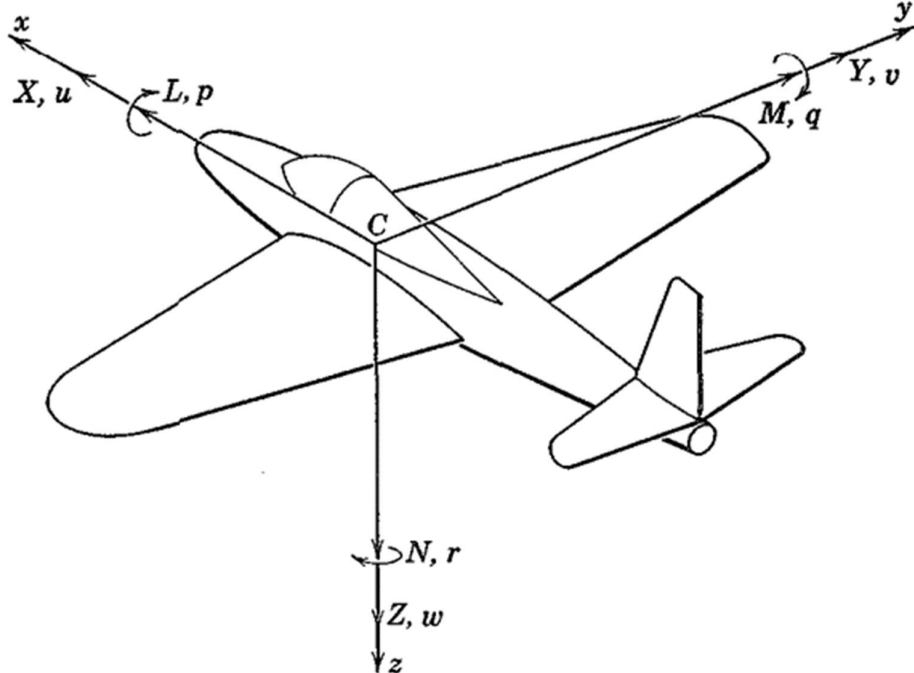


Figure 11. Notation of body-fixed frame

Table 1. Notation names of body-fixed frame

Moments	Aerodynamic Forces	Rates	Velocities
L, Rolling Moment	X	p	u
M, Pitching Moment	Y	q	v
N, Yawing Moment	Z	r	w

2.1.2 Frame Rotation

Rotations can be performed between coordinate systems, allowing parameters calculated in one coordinate system to be utilized in another. As these matrices are orthogonal, their inverse is equal to their transpose. Consequently, when one wishes to revert from a transformed coordinate system back to the original, multiplying the transformation matrix by its transpose is sufficient. This property allows smooth transitions between coordinate systems, ensuring compatibility and accuracy in parameter calculations across different frames.

The following operations can be performed to convert from wind fixed frame (F_W) to body fixed frame (F_B).

- Rotation around the z_w -axis of wind fixed axis by the $-\beta$ angle (defined as the sideslip angle),
- Rotation around the newly formed y' -axis by angle α (defined as the angle of attack),
- There is no need for any rotation around the z -axis.

This frame transformation can be expressed mathematically with transformation matrices as given below.

$$\begin{bmatrix} x_B \\ y_B \\ z_B \end{bmatrix} = \begin{bmatrix} \cos(\alpha) & 0 & -\sin(\alpha) \\ 0 & 1 & 0 \\ \sin(\alpha) & 0 & \cos(\alpha) \end{bmatrix} \begin{bmatrix} \cos(-\beta) & \sin(-\beta) & 0 \\ -\sin(-\beta) & \cos(-\beta) & 0 \\ 0 & 0 & 1 \end{bmatrix} \begin{bmatrix} x_w \\ y_w \\ z_w \end{bmatrix}$$

2.1.3 Forces and Moments

The forces and moments acting on an aircraft are generally defined on the Body Fixed Reference Frame. The forces acting on the aircraft can be seen in Figure 12.

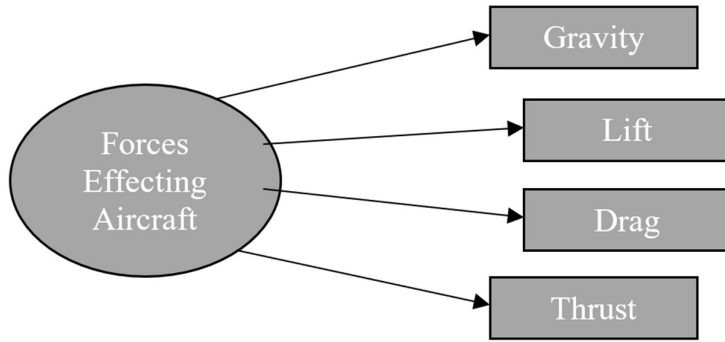


Figure 12. Forces effecting the aircraft

These aerodynamic forces (except gravity) and the resulting moments are generally named with a letter according to their effects on the body fixed reference frame in aircraft. As seen in Table 1, instead of total forces, they are evaluated by separating the components in each axis.

2.1.4 Angles, Angular Velocity and Rates

The alignment between one reference frame and another can be described through three angles. These angles represent sequential rotations about the z, y, and x axes, respectively, bringing one frame into alignment with the other. This concept is a specific instance of Euler angles. The angles are denoted (Ψ, θ, Φ) for body axes and $(\Psi_W, \theta_W, \Phi_W)$ for wind axes.

- A rotation around z-axis of Vehicle Carried Frame represented as Ψ , called as azimuth angle.
- A rotation around y-axis of newly formed frame represented as θ , called as elevation angle.
- A rotation around x-axis of newly formed frame represented as Φ , called as bank angle.

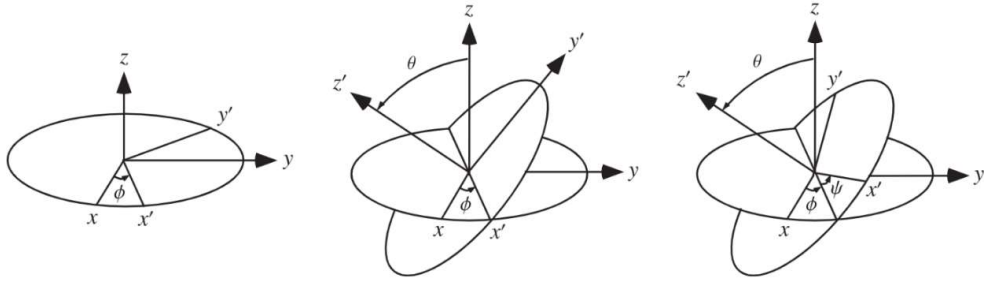


Figure 13. Euler angles

Within the body-fixed frame, the translational motion of the aircraft can be denoted as a vector V , encompassing its u , v , and w components. Furthermore, this motion can be characterized by the magnitude of V and two appropriate angles. Those angles which called angle of attack α (AOA) and sideslip angle β (SSA) are defined respect to velocity components:

$$\alpha = \tan^{-1} \frac{w}{u}$$

$$\beta = \sin^{-1} \frac{v}{V}$$

AOA measures the slope of the wing surface against the airflow and is usually expressed in degrees or radians. SSA is a measure of how much the nose of the aircraft deviates laterally from the direction of the airflow. It gauges the lateral sliding motion induced by crosswinds, or other factors arising from the flight condition of the aircraft.

The angular velocity components (p, q, r) in body axes are measured by body-fixed sensors. Conversion is needed to achieve Euler angle velocities $(\dot{\psi}, \dot{\theta}, \dot{\phi})$.

$$\dot{\phi} = p + \tan\theta(q\sin\phi + r\cos\phi)$$

$$\dot{\theta} = q\cos\phi - r\sin\phi$$

$$\dot{\psi} = \sec\theta (q\sin\phi + r\cos\phi)$$

2.1.5 6-DOF Equations of Motions

Some presuppositions are made before obtaining the equations. These can be expressed as follows, the equations are written as the plane of symmetry of the aircraft,

the XZ plane. And the equations are written for the body-fixed reference frame of the aircraft. These equations of motions are same for all aircraft. By applying the calculated forces and moments to these equations, the state of the aircraft is obtained. Since the equations of motion are calculated according to the body axis set, the forces and moments obtained must be converted to the body axis set if they are not calculated in the body axis set. Three of these degrees of freedom represent translational dynamics, while the other three represent rotational dynamics.

2.1.5.1 3-DoF Translational Equations

It can be expressed as linear movements made by the aircraft. These movements made according to the body-fixed axis set can be expressed with u, v, w as shown in Table 1. When equations begin to be created according to Newton's Second Law:

$$F = ma = m \frac{d}{dt} V_t = \frac{d}{dt} V_t (mV_t)$$

Here F represents the sum of all external forces acting on the aircraft and V_t represents translational velocity in body axis reference frame. Then, when we organize the equations by including the angular positions and angular velocities of the aircraft into the equation, we can write following equations.

$$\begin{aligned}\dot{u} &= \frac{\sum F_x}{m} + (-qw + rv) \\ \dot{v} &= \frac{\sum F_y}{m} + (-ur + pw) \\ \dot{w} &= \frac{\sum F_z}{m} + (-pv + qu)\end{aligned}$$

2.1.5.2 3-DoF Rotational Equations

It refers to the rotational movements of the aircraft according to the body fixed reference frame. As shown in Table 1, movements in this period can be expressed as p, q, r . We can write the angular momentum equation as given below.

$$H = I\omega$$

Inertia matrix represented as follows.

$$I = \begin{bmatrix} I_{xx} & -I_{xy} & -I_{xz} \\ -I_{xy} & I_{yy} & -I_{yz} \\ -I_{xz} & -I_{yz} & I_{zz} \end{bmatrix}$$

H which is represented as angular momentum matrix, equals as follows.

$$H = \begin{bmatrix} I_{xx} & -I_{xy} & -I_{xz} \\ -I_{xy} & I_{yy} & -I_{yz} \\ -I_{xz} & -I_{yz} & I_{zz} \end{bmatrix} \begin{bmatrix} p \\ q \\ r \end{bmatrix}$$

Therefore, the angular acceleration can be expressed as follows.

$$\dot{H} = \begin{cases} \dot{H}_x = I_{xx}\dot{p} - I_{xy}\dot{q} - I_{xz}\dot{r} \\ \dot{H}_y = -I_{xy}\dot{p} + I_{yy}\dot{q} - I_{yz}\dot{r} \\ \dot{H}_z = -I_{xz}\dot{p} - I_{yz}\dot{q} + I_{zz}\dot{r} \end{cases}$$

Sum of all externally applied moments can be found as follows. Moments are summed about the center of mass of the aircraft.

$$M = \frac{d}{dt} H + \omega * H = \frac{d}{dt} I\omega + \omega * H$$

If we substitute what we found into the equation, we can obtain the following equations.

$$M = (\dot{H}_x i_B + \dot{H}_y j_B + \dot{H}_z k_B) + \begin{vmatrix} i_B & j_B & k_B \\ p & q & r \\ H_x & H_y & H_z \end{vmatrix}$$

$$\begin{aligned} M = & ([I_{xx}\dot{p} - I_{xy}\dot{q} - I_{xz}\dot{r}]i_B + [-I_{xy}\dot{p} + I_{yy}\dot{q} - I_{yz}\dot{r}]j_B + [-I_{xz}\dot{p} - I_{yz}\dot{q} + I_{zz}\dot{r}]k_B \\ & + [qH_z - rH_y]i_B + [rH_x - pH_z]j_B + [pH_y - qH_x]k_B) \end{aligned}$$

$$M = L * i_B + M * j_B + N * k_B$$

Since $I_{xy} = I_{yz} = 0$ because of symmetrical plane of aircraft, 3-DoF Rotational equations can be written as follows.

$$L = I_{xx}\dot{p} - I_{xz}(\dot{r} + pq) + (I_{zz} - I_{yy})qr$$

$$M = I_{yy}\dot{q} - I_{xz}(p^2 - r^2) + (I_{xx} - I_{zz})pr$$

$$N = I_{zz}\dot{r} - I_{xz}p + pq(I_{yy}-I_{xx}) + I_{xz}qr$$

2.1.6 Translational Kinematics

It is formed by expressing the translational movements of the aircraft in an earth fixed reference frame. Also called flight path equations. When velocity components shown for the Body fixed reference frame in Table 1 are used to obtain equations, axis transformations must be made using Euler angles. To transform from Body Fixed frame to Earth Fixed Frame, the transformation matrix that is given below should be used.

$$\begin{bmatrix} \dot{x} \\ \dot{y} \\ \dot{z} \end{bmatrix} = T_B^E \begin{bmatrix} u \\ v \\ w \end{bmatrix}$$

Here,

$$T_B^E = \begin{bmatrix} \cos\psi \cos\theta & \cos\psi \sin\theta \sin\phi - \sin\psi \cos\theta & \cos\psi \sin\theta \cos\phi + \sin\psi \sin\phi \\ \sin\psi \cos\theta & \sin\psi \sin\theta \sin\phi + \cos\psi \cos\theta & \sin\psi \sin\theta \cos\phi - \cos\psi \sin\phi \\ -\sin\theta & \cos\theta \cos\phi & \cos\theta \cos\phi \end{bmatrix}$$

To create translational kinematics equations, body frame components and earth frame can be expressed as follows.

$$V = i_B u + j_B v + k_B w \quad V_{ground} = i_e \dot{x} + j_e \dot{y} + k_e \dot{z}$$

As a result, the translational kinematic equations are represented as follows.

$$\begin{aligned} \dot{x} &= u(\cos\psi \cos\theta) + v(\cos\psi \sin\theta \sin\phi - \sin\psi \cos\theta) + w(\cos\psi \sin\theta \cos\phi + \sin\psi \sin\phi) \\ \dot{y} &= u(\sin\psi \cos\theta) + v(\sin\psi \sin\theta \sin\phi + \cos\psi \cos\theta) + w(\sin\psi \sin\theta \cos\phi - \cos\psi \sin\phi) \\ \dot{z} &= u(-\sin\theta) + v(\cos\theta \cos\phi) + w(\cos\theta \cos\phi) \end{aligned}$$

2.1.7 Rotational Kinematics

Rotational kinematics are formed by expressing the rotational movements of the aircraft. When rotational velocity components shown for the Body-fixed reference frame in Table 1 are used to obtain equations, conversion should be made by using Euler angles.

$$\begin{bmatrix} p \\ q \\ r \end{bmatrix} = \begin{bmatrix} 1 & 0 & -\sin\theta \\ 0 & \cos\phi & \sin\phi \cos\theta \\ 0 & -\sin\phi & \cos\phi \cos\theta \end{bmatrix} \begin{bmatrix} \dot{\phi} \\ \dot{\theta} \\ \dot{\psi} \end{bmatrix}$$

To obtain Euler angle acceleration, the inverse of matrix is used.

$$\begin{bmatrix} \dot{\phi} \\ \dot{\theta} \\ \dot{\psi} \end{bmatrix} = \begin{bmatrix} 1 & \tan\theta \sin\phi & \cos\phi \tan\theta \\ 0 & \cos\phi & -\sin\phi \\ 0 & \sec\theta \sin\phi & \sec\theta \cos\phi \end{bmatrix} \begin{bmatrix} p \\ q \\ r \end{bmatrix}$$

As a result, the kinematic equations can be expressed as follows.

$$\begin{aligned} \dot{\phi} &= p + \tan\theta(q\sin\phi + r\cos\phi) \\ \dot{\theta} &= q\cos\phi - r\sin\phi \\ \dot{\psi} &= \sec\theta(q\sin\phi + r\cos\phi) \end{aligned}$$

2.2 Trim and Linearization

2.2.1 Trim Definition and Purpose

Trim refers to the adjustments made on an aircraft to maintain a stable condition during flight. The trim setting involves setting the positions of control surfaces (ailerons, elevators, rudder, etc.) and engine power to specific values. These adjustments allow the aircraft to fly at a certain speed and altitude with minimal manual input from the pilot.

During flight, trimming an aircraft is essential to keep it in a specific position and speed. Without trim adjustments, the pilot may need to continuously adjust control surfaces manually, leading to a tiring and unstable flight.

2.2.2 Linearization

The flight dynamics of aircraft are typically expressed by nonlinear equations. However, flight control systems are often designed using linear models, necessitating the process of linearization.

Linearization involves transforming a nonlinear system into a linear model at a specific operating point (referred to as the trim point). The trim point represents a stable state

where the aircraft flies at a particular altitude, speed, and other parameters. Linearization is carried out at this trim point. The steps for linearization are as follows.

- Determining the Trim Point: Identification of the trim point where the aircraft is flying stably under specific flight conditions.
- Calculating Linearization Matrices: The nonlinear equations around the trim point are linearized using Taylor series, resulting in the computation of linearization matrices (A, B, C, D system matrices).
- Linear Control System Design: Designing a linear control system based on the linearized model.
- Application and Adjustments: Implementing the designed linear control system into the aircraft's flight control system and making necessary adjustments.

These steps are crucial for incorporating linearization and trim processes in the design and development of flight control systems, ensuring the aircraft's stable and secure flight.

2.2.3 Trim Conditions

Trim point varies under different constraints and flight conditions. Generally, four main categories of trim conditions are examined, encompassing straight and level flight, pull-up/push-over maneuvers, steady-state turns, and steady heading sideslips.

- Straight and Level Flight

This scenario aims to establish a stable equilibrium point for the aircraft in straight and level horizontal flight with any horizontal velocity and any pitch angle.

When determining the trim point, it focuses on achieving a state where the aerodynamic forces and moments in horizontal and vertical components are balanced.

- Pull-up / Push-over Maneuvers

This situation involves the vertical motion of the aircraft. In pull-up, considerations include vertical velocity and altitude gain, while in push-over, vertical velocity and altitude loss are considered.

Establishing the trim point involves balancing the vertical motion and associated moments.

➤ *Steady-state Turn*

In a coordinated turn, the goal is to maintain the aircraft at a specific horizontal speed and bank angle in a stable condition.

Trim conditions include achieving a balance where the turn rate, bank angle, and relevant moments are fixed.

➤ *Steady Heading Sideslip*

With a fixed heading, the objective is for the aircraft to maintain stability at a specific horizontal speed and a particular sideslip angle.

Trim conditions involve fixing the sideslip angle and heading angle while considering the aerodynamic interactions.

The trim conditions examined under these four main categories are essential for identifying equilibrium points suitable for different flight situations. Each condition aims to analyze the aerodynamic behavior of the aircraft in detail, providing critical insights for optimizing flight performance.

The GTM aircraft is trimmed around 500 ft altitude, 75 kts True Airspeed and -3° Gamma angle. Linearization is performed at this trim point.

System matrix is as follows.

$$\begin{bmatrix} \dot{TAS} \\ \alpha \\ \beta \\ \dot{p} \\ \dot{q} \\ \dot{r} \\ Lat \\ Lon \\ Alt \\ \dot{\phi} \\ \dot{\theta} \\ \dot{\psi} \end{bmatrix} = \begin{bmatrix} -0.07249 & -15.11 & -0.01603 & -4.383e-07 & 0.2601 & -2.068e-07 & 0 & 0 & 2.94e-05 & -0.003069 & -32.13 & 0 & TAS \\ -0.003961 & -2.333 & -0.0009205 & 4.105e-08 & 0.9443 & 1.687e-08 & 0 & 0 & 7.474e-06 & -0.0002412 & 0.0133 & 0 & \alpha \\ -3.831e-06 & -0.002476 & -0.4955 & 0.1008 & 4.081e-13 & -0.9837 & 0 & 0 & 7.119e-09 & 0.2539 & -1.16e-05 & 0 & \beta \\ -3.081e-05 & -0.1705 & -81.57 & -5.68 & -0.02734 & 2.225 & 0 & 0 & -1.345e-08 & 0 & 0 & 0 & p \\ -0.006206 & -38.93 & 0.6654 & -0.006125 & -3.248 & 0.0379 & 0 & 0 & -2.71e-06 & 0 & 0 & 0 & q \\ -1.511e-06 & -0.005873 & 25.62 & -0.4789 & -0.03053 & -1.322 & 0 & 0 & -6.595e-10 & 0 & 0 & 0 & r \\ 4.575e-12 & 5.755e-09 & -6.056e-06 & 0 & 0 & 0 & 0 & 0 & -2.771e-17 & 6.056e-07 & 4.215e-14 & -6.048e-06 & Lat \\ 6.049e-08 & -4.013e-07 & 3.509e-10 & 0 & 0 & 0 & 5.946e-06 & 0 & -3.664e-13 & -3.509e-11 & 4.013e-07 & 7.332e-10 & Lon \\ -0.05234 & -126.4 & -0.1207 & 0 & 0 & 0 & 0 & 0 & 0 & 0.01207 & 126.4 & 0 & Alt \\ 0 & 0 & 0 & 1 & 4.569e-05 & 0.04784 & 0 & 0 & 0 & 1.692e-08 & -8.665e-11 & 0 & \Phi \\ 0 & 0 & 0 & 0 & 1 & -0.000955 & 0 & 0 & 0 & 8.646e-11 & 0 & 0 & \Theta \\ 0 & 0 & 0 & 0 & 0.0009561 & 1.001 & 0 & 0 & 0 & 3.541e-07 & -4.141e-12 & 0 & \Psi \end{bmatrix}$$

$$+ \begin{bmatrix} -0.03365 & 0.03299 & -0.005254 & -0.008726 & -0.008726 & -0.1191 & -0.05011 & 0.06068 & 0.06068 \\ -0.004045 & -0.001163 & -0.0004744 & 0.001515 & 0.001515 & -0.004786 & -0.006364 & -6.472e-05 & -6.472e-05 \\ -5.28e-14 & -0.0001306 & 0.002901 & 7.922e-05 & 7.922e-05 & -1.869e-13 & -7.864e-14 & 9.963e-06 & 9.963e-06 \\ -0.003603 & -0.7816 & 0.1985 & -0.4239 & -0.4239 & 0.0002258 & -0.004977 & 0.008389 & 0.008389 \\ -0.7257 & -0.08178 & -0.002501 & 0.01298 & 0.01298 & 0.04548 & -1.003 & 0.008218 & 0.008218 \\ -0.0001766 & -0.04701 & -0.3927 & -0.04815 & -0.04815 & 1.107e-05 & -0.000244 & 0.02384 & 0.02384 \\ 0 & 0 & 0 & 0 & 0 & 0 & 0 & 0 & 0 \\ 0 & 0 & 0 & 0 & 0 & 0 & 0 & 0 & 0 \\ 0 & 0 & 0 & 0 & 0 & 0 & 0 & 0 & 0 \\ 0 & 0 & 0 & 0 & 0 & 0 & 0 & 0 & 0 \\ 0 & 0 & 0 & 0 & 0 & 0 & 0 & 0 & 0 \end{bmatrix} \begin{bmatrix} Elevator \\ Aileron \\ Rudder \\ L Spoiler \\ R Spoiler \\ Flaps \\ Stabilizer \\ L Throttle \\ R Throttle \end{bmatrix}$$

2.3 Aircraft Modes

Aircraft modes are essential elements in understanding and controlling the dynamic behavior of an aircraft. Longitudinal modes, focusing on the aircraft's longitudinal motion, include the Phugoid mode, by pitch oscillations, and the Short-Period mode, depicting rapid pitch fluctuations influenced by instantaneous control inputs. On the other hand, lateral-directional modes encompass the Roll mode, which highlights lateral rolling motion, the Dutch-Roll mode, a lateral oscillation with yawing, and the Spiral mode, representing coordinated horizontal turns.

Understanding these modes is crucial for optimizing flight performance and stability, making them integral to the fields of flight engineering and control system design. Each mode interacts with factors such as aerodynamics, mass distribution, control surfaces, and engine thrust, emphasizing the close relationship between these elements. This comprehensive analysis of aircraft modes is pivotal for the effective optimization of flight dynamics and safety.

2.3.1 Longitudinal Modes

Overall system matrix is obtained in section 2.2.3. Longitudinal system matrix is given below.

$$\begin{bmatrix} \dot{TAS} \\ \dot{\alpha} \\ \dot{q} \\ \dot{\theta} \end{bmatrix} = \begin{bmatrix} -0.07249 & -15.11 & 0.2601 & -32.13 \\ -0.003961 & -2.333 & 0.9443 & 0.0133 \\ -0.006206 & -38.93 & -3.248 & 0 \\ 0 & 0 & 1 & 0 \end{bmatrix} \begin{bmatrix} TAS \\ \alpha \\ q \\ \theta \end{bmatrix} + \begin{bmatrix} -0.03365 & 0.06068 \\ -0.004045 & -6.472e-05 \\ -0.7257 & 0.008218 \\ 0 & 0 \end{bmatrix} \begin{bmatrix} Elevator \\ Throttle \end{bmatrix}$$

Longitudinal modes serve as a fundamental reference point for understanding an aircraft's longitudinal motion. These modes represent the pitch (nose up-down) movements of the aircraft and typically encompass two main modes: the Phugoid mode and the Short-Period mode.

2.3.1.1 Phugoid mode

The Phugoid mode, representing the longitudinal motion of an aircraft, is characterized by the oscillation of pitch. This mode is associated with long-period, quasi-static motions where the aircraft alternately climbs and descends like in Figure 14. It is crucial for understanding the energy exchange between potential and kinetic energy during flight. Factors influencing Phugoid mode stability include the aircraft's mass distribution, aerodynamic properties, and the effectiveness of the control system. Phugoid mode properties are given in Table 2.

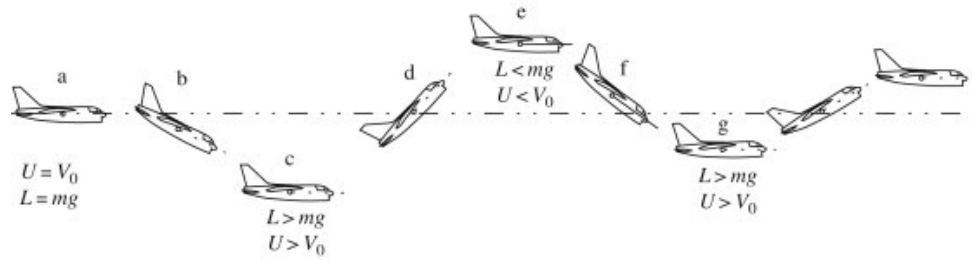


Figure 14. Phugoid mode effect on aircraft

Table 2. Phugoid mode properties

Root Location	Natural Frequency	Damping Ratio	Period
-0.022234±0.30826i	0.30906	0.07194	20.33

2.3.1.2 Short-period mode

Short-Period mode is characterized by rapid, short-duration oscillations primarily in pitch as given in Figure 15. These oscillations are often a result of sudden and pronounced control inputs, demonstrating the aircraft's immediate response to pilot commands. The Short-Period mode is influenced by parameters such as aircraft mass, aerodynamic characteristics, and the agility of the control system. Short-period mode properties are given in Table 3.

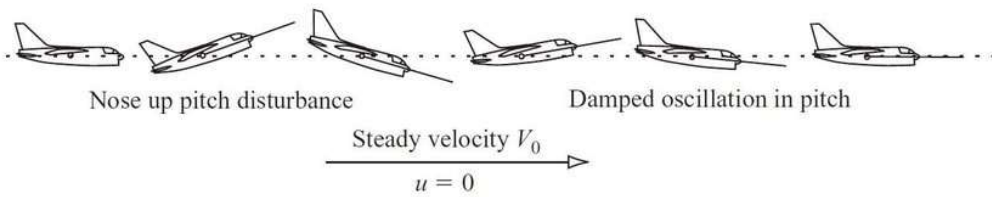


Figure 15. Short-period mode effect on aircraft

Table 3. Short-period mode properties

Root Location	Natural Frequency	Damping Ratio	Period
-2.7614±6.0102i	6.6142	0.41749	0.94995

2.3.2 Lateral-directional Modes

Lateral system matrix is given below.

$$\begin{bmatrix} \dot{\beta} \\ \dot{p} \\ \dot{r} \\ \dot{\phi} \end{bmatrix} = \begin{bmatrix} -0.4955 & 0.1008 & -0.9837 & 0.2539 \\ -81.57 & -5.68 & 2.225 & 0 \\ 25.62 & -0.4789 & -1.322 & 0 \\ 0 & 1 & 0.04784 & 1.692e-08 \end{bmatrix} \begin{bmatrix} \beta \\ p \\ r \\ \phi \end{bmatrix} \\ + \begin{bmatrix} -0.0001306 & 0.002901 \\ -0.7816 & 0.1985 \\ -0.04701 & -0.3927 \\ 0 & 0 \end{bmatrix} \begin{bmatrix} \text{Aileron} \\ \text{Rudder} \end{bmatrix}$$

Lateral-directional modes hold fundamental significance in understanding the lateral (sideways) and directional movements of an aircraft. These modes encompass the Roll mode, Dutch-Roll mode, and Spiral mode.

2.3.2.1 Roll mode

Roll mode focuses on the lateral motion of an aircraft, particularly its rolling motion about the longitudinal axis. This mode arises from imbalances in lift between the wings due to a lateral displacement of the center of gravity. Roll mode stability and response are closely tied to aeroelastic properties, the configuration of control surfaces, and the overall geometry of the aircraft. Roll mode effect on aircraft is given in Figure 16 and properties are given in Table 4.

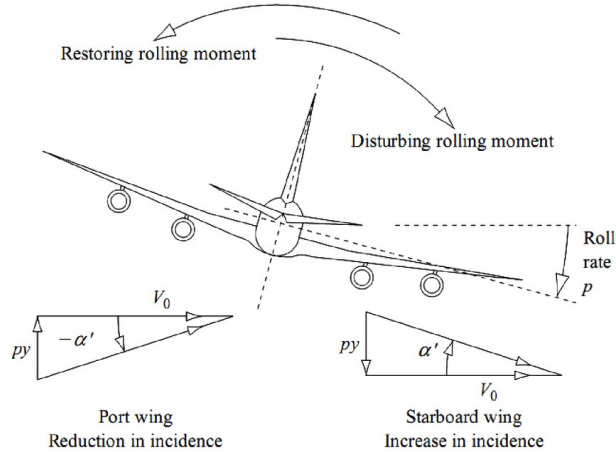


Figure 16. Roll mode effect on aircraft

Table 4. Roll mode properties

Root Location	Natural Frequency	Time Constant
-5.8107	5.8107	0.1721

2.3.2.2 Dutch-roll mode

Dutch-Roll mode involves a combination of lateral oscillation and yawing motion as seen in Figure 17. It is a lateral stability mode that manifests as an alternating side-to-side motion. The Dutch-Roll mode's stability is dependent on the coordination and interaction between the aircraft's vertical and lateral stability controls. Dutch-roll mode properties are given in Table 5.

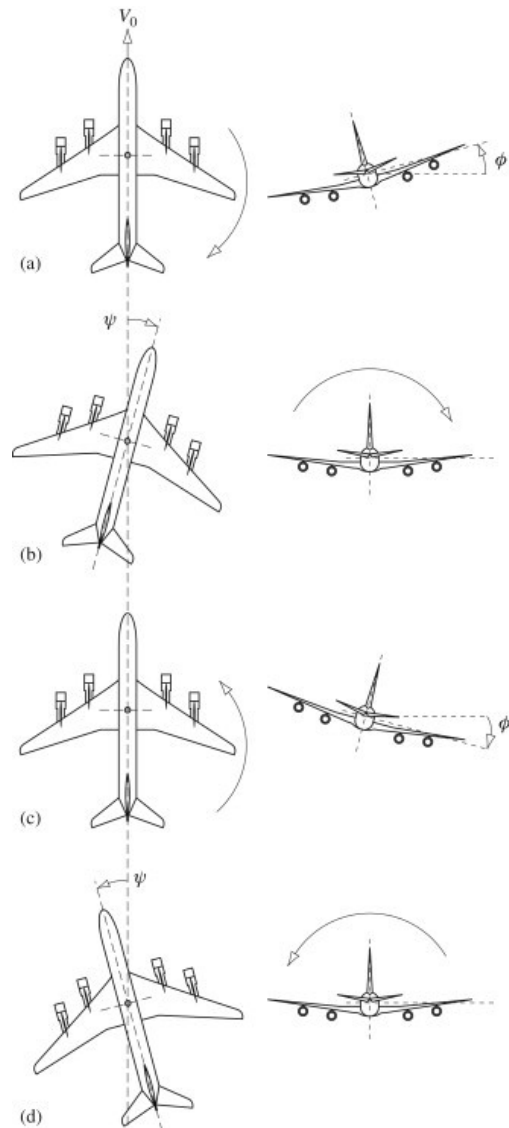


Figure 17. Dutch-roll mode effect on aircraft

Table 5. Dutch-roll mode properties

Root Location	Natural Frequency	Damping Ratio	Period
-0.79505±5.8963i	5.9497	0.13363	1.0561

2.3.2.3 Spiral mode

Spiral mode represents a horizontal, coordinated turn of an aircraft. It influences lateral stability and occurs when the aircraft tends to roll and yaw simultaneously as seen in Figure 18. The stability of the Spiral mode is influenced by vertical stability controls, engine thrust, and other aerodynamic factors. Spiral mode properties are given in Table 6.

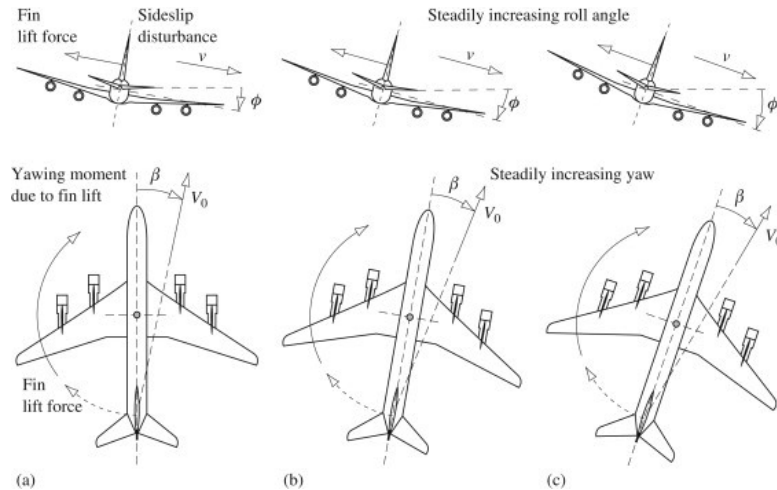


Figure 18. Spiral mode effect on aircraft

Table 6. Spiral mode properties

Root Location	Natural Frequency	Time Constant
-0.039425	0.039425	25.364

These detailed descriptions provide a comprehensive overview of each mode, offering insight into their characteristics and the factors influencing their stability in the context of aircraft dynamics.

3 LANDING PHASES

3.1 Base Leg

The Base Leg is a crucial phase during the aircraft landing sequence, characterized by a horizontal flight path that aligns the aircraft with the intended runway. This segment allows the autopilot to establish the proper approach angle and prepare for the subsequent descent. It serves as a transitional phase, linking the initial descent from the traffic pattern to the final approach for landing as seen in Figure 19.

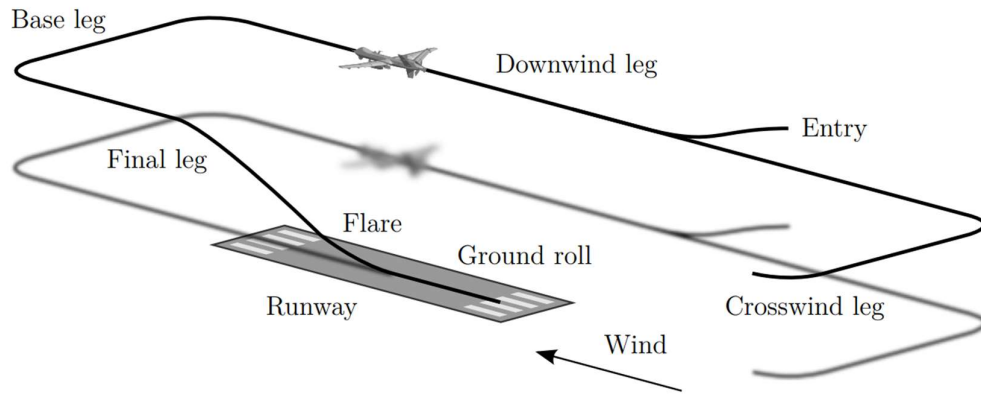


Figure 19. Landing phases

3.2 Glide

The Glide, namely final approach-leg, involves a controlled descent of the aircraft along a predefined approach path towards the runway. During this stage engine power is reduced, the aircraft maintains a stabilized descent rate and adjusts the pitch attitude and airspeed to ensure precise alignment with the runway's extended centerline. Additionally, opening the landing gear and flaps helps reduce airspeed. The Glide phase represents a critical component of the landing process, requiring the pilot's or autopilot's careful management of altitude, airspeed, and descent angle.

3.3 Flare

The Flare phase is the critical moment just before touchdown when the autopilot initiates a gentle pitch-up maneuver to arrest the descent rate and transition from a descent to a level attitude. This phase is essential for achieving a smooth and controlled landing. To ensure this, engine power, flaps, air brakes and landing gear must be

controlled intelligently. The autopilot carefully adjusts the pitch attitude to "flare" the aircraft, gradually reducing the descent rate to facilitate a soft and safe touchdown on the runway as seen in Figure 20.

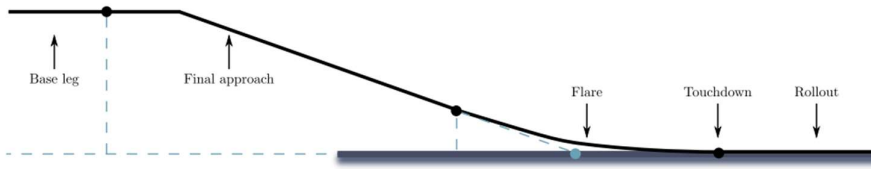


Figure 20. Flare maneuver for soft and safe touchdown

3.4 Touchdown

Touchdown marks the point at which the aircraft's wheels contact the runway surface. The objective during this phase is to execute a smooth and controlled landing, minimizing any vertical or lateral oscillations. Autopilots strive for a main gear first touchdown, distributing the weight evenly across the landing gear and optimizing aircraft control during the rollout.

3.5 Taxi

The Taxi phase involves the aircraft's movement on the ground after landing, as it navigates from the runway to the designated parking or terminal area. Autopilot follows taxiway instructions and ground control guidance to ensure the safe and efficient movement of the aircraft on the airport surface. This phase includes considerations such as engine power settings, braking, and adherence to airport signage and markings.

4 OPEN-LOOP ANALYSIS

The GTM aircraft is trimmed for landing and linearization is performed around the trim point as mentioned at section 2.2.

Trim point is given in Table 7.

Table 7. Trim point

Altitude	True Airspeed	Gamma Angle
500 ft	75 kts	-3°

To validate the accuracy of the linearization process, identical inputs are applied to both linear and nonlinear systems, and their corresponding outputs are observed. Doublet inputs are separately administered to the elevator, aileron, and rudder control surfaces.

For elevator input, the outputs of pitch rate (q) and pitch angle (θ) are examined. Aileron input resulted in outputs of roll rate (p) and roll angle (ϕ). Rudder input led to outputs of yaw rate (r) and azimuth angle (ψ). Additionally, longitudinal speed (u), lateral speed (v), and vertical speed (w) are examined for each input. Special attention is given to ensuring that the output values are consistent with the initial values under trim conditions. Angular velocities and rates according to elevator, aileron, and rudder doublets are given in Figure 21 and linear velocities are given in Figure 22.

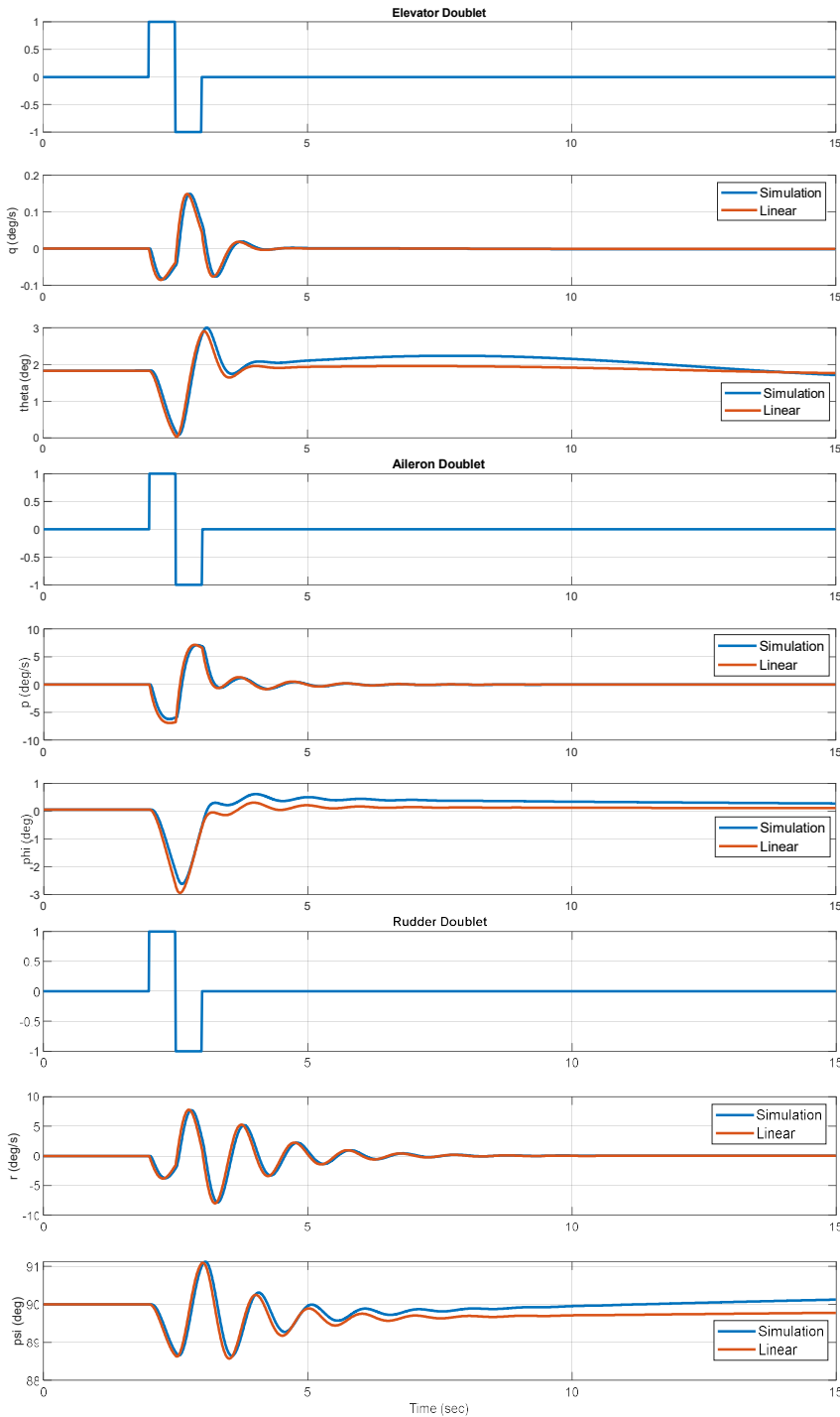


Figure 21. Angular velocities and rates according to control surfaces doublets

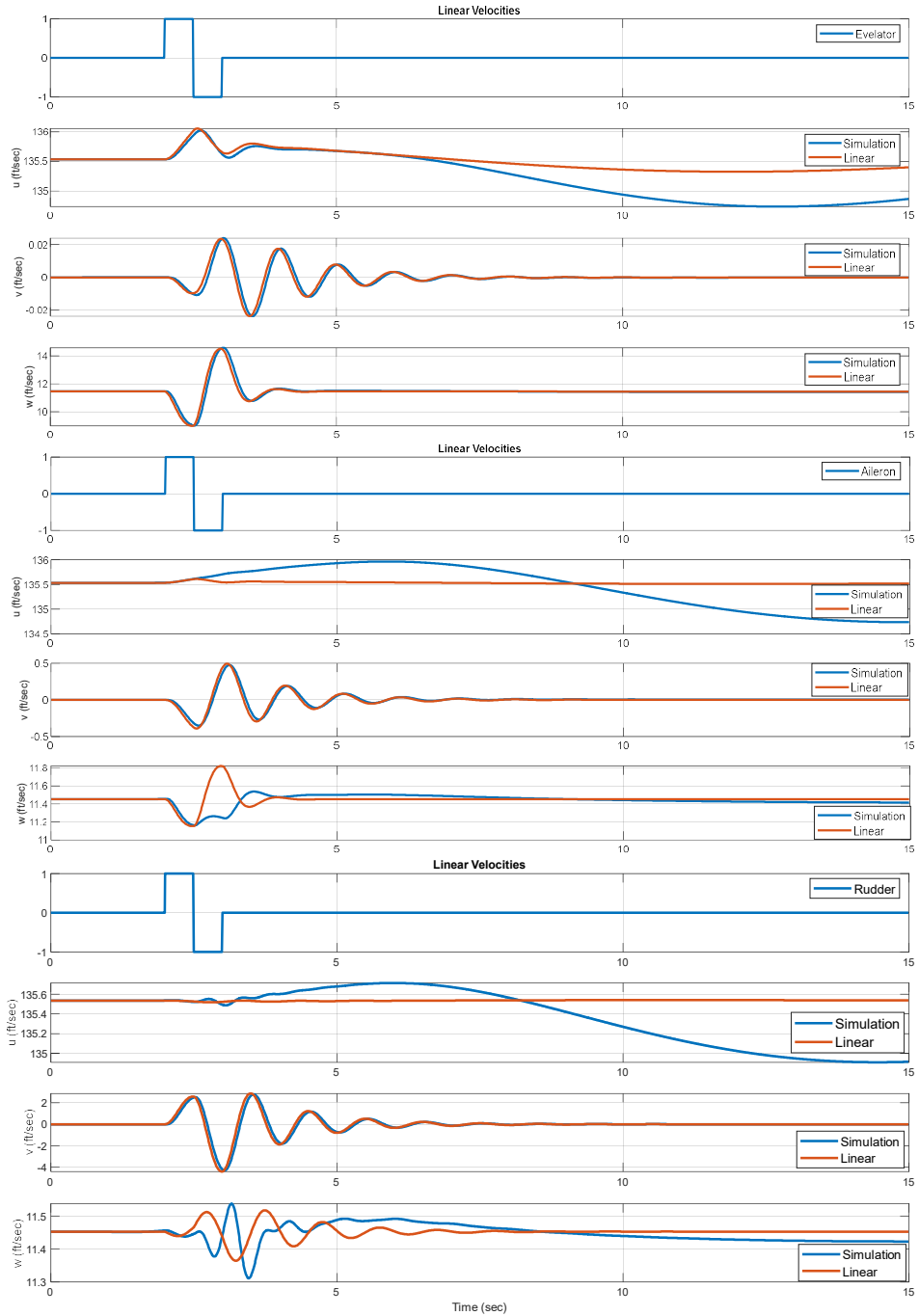


Figure 22. Linear velocities according to control surfaces doublets

4.1 Transfer Functions

4.1.1 Transfer Functions of Elevator

The elevator, situated on the horizontal stabilizer of an aircraft, plays a crucial role in controlling the pitch motion of the aircraft. It significantly influences the angle of

attack (AOA), pitch attitude, and pitch rate, thereby playing a critical role in managing the longitudinal stability and maneuverability of the aircraft.

$$\triangleright \frac{\partial \theta}{\partial \text{Elevator}} = \frac{-0.78445 (s+2.272)(s+0.05242)}{(s^2 + 0.05904s + 0.08882)(s^2 + 6.05s + 51.46)}$$

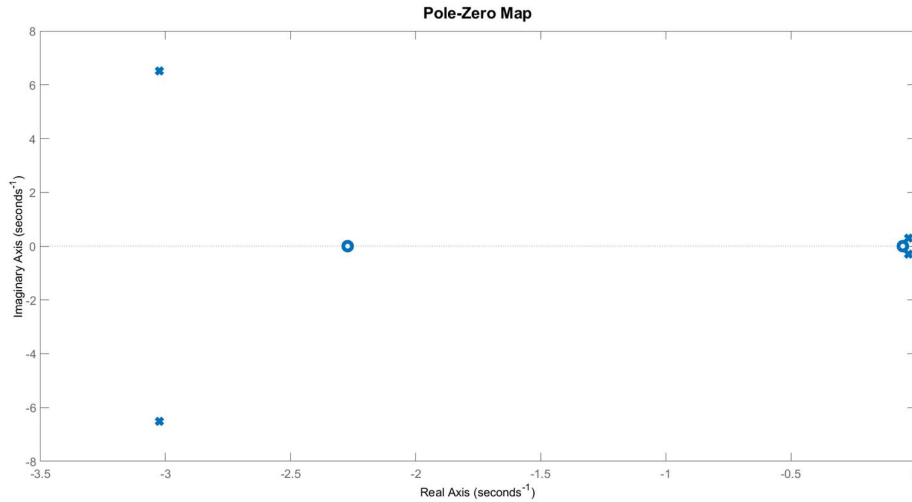


Figure 23. Pole-Zero Map of $\frac{\partial \theta}{\partial \text{Elevator}}$

$$\triangleright \frac{\partial q}{\partial \text{Elevator}} = \frac{-0.78445 (s+2.272)(s+0.05214)(s+2.129e-05)}{(s^2 + 0.05904s + 0.08882)(s^2 + 6.05s + 51.46)}$$

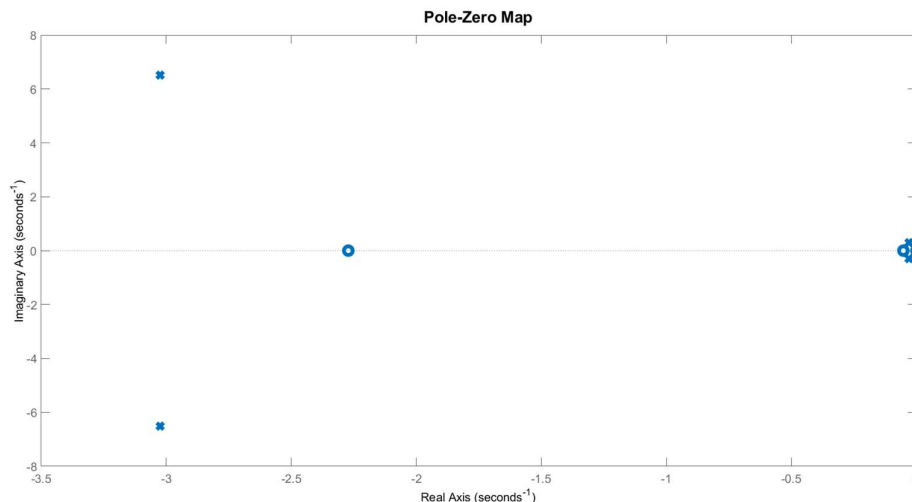


Figure 24. Pole-Zero Map of $\frac{\partial q}{\partial \text{Elevator}}$

4.1.2 Transfer Functions of Aileron

Ailerons, typically positioned near the wingtips, operate differentially to govern the roll motion of the aircraft. They affect the roll rate, bank angle, and lateral stability, facilitating the aircraft's rolling and aiding in turn execution.

$$\Rightarrow \frac{\partial \phi}{\partial Ail} = \frac{-0.94799 (s^2 + 2.052s + 35.47)}{(s+6.594)(s+0.05541)(s^2 + 1.707 + 39.95)}$$

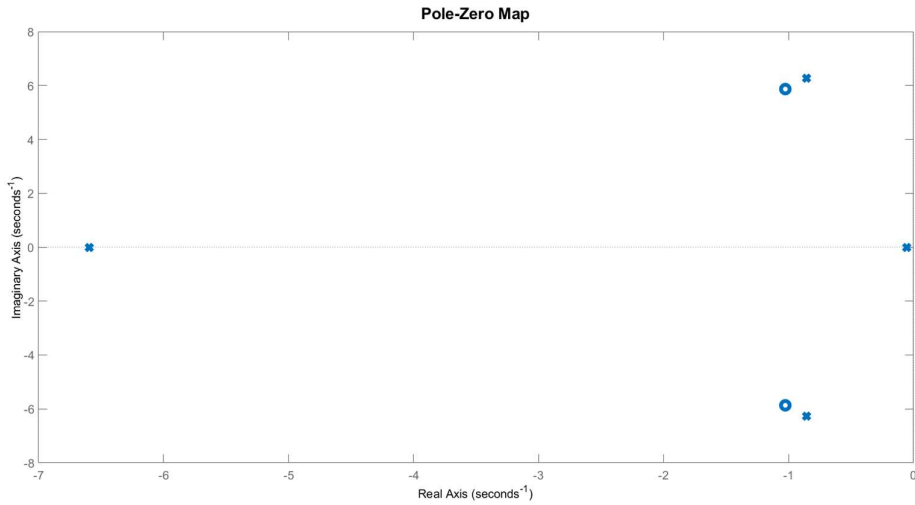


Figure 25. Pole-Zero Map of $\frac{\partial \phi}{\partial \text{Aileron}}$

$$\Rightarrow \frac{\partial p}{\partial Ail} = \frac{-0.94626 (s-0.007489)(s^2 + 2.066s + 35.45)}{(s+6.594)(s+0.05541)(s^2 + 1.707s + 39.95)}$$

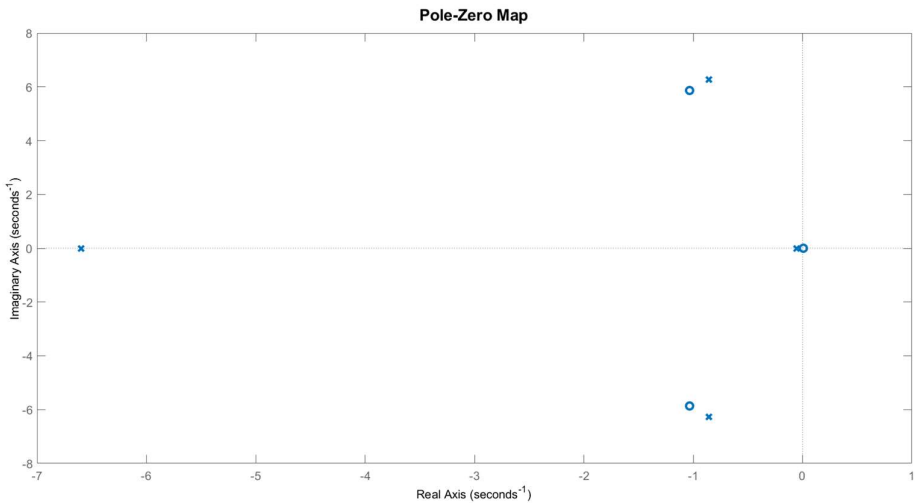


Figure 26. Pole-Zero Map of $\frac{\partial p}{\partial \text{Aileron}}$

4.1.3 Transfer Functions of Rudder

The rudder, commonly located on the vertical stabilizer of the aircraft, is employed to control the yaw motion. It impacts the yaw rate, heading angle, and directional stability, contributing to coordinated turns and mitigating adverse yaw effects.

$$\Rightarrow \frac{\partial \beta}{\partial \text{Rud}} = \frac{0.003102 (s+152.2)(s+6.432)(s-0.05548)}{(s+6.594)(s+0.05541)(s^2 + 1.707s + 39.95)}$$

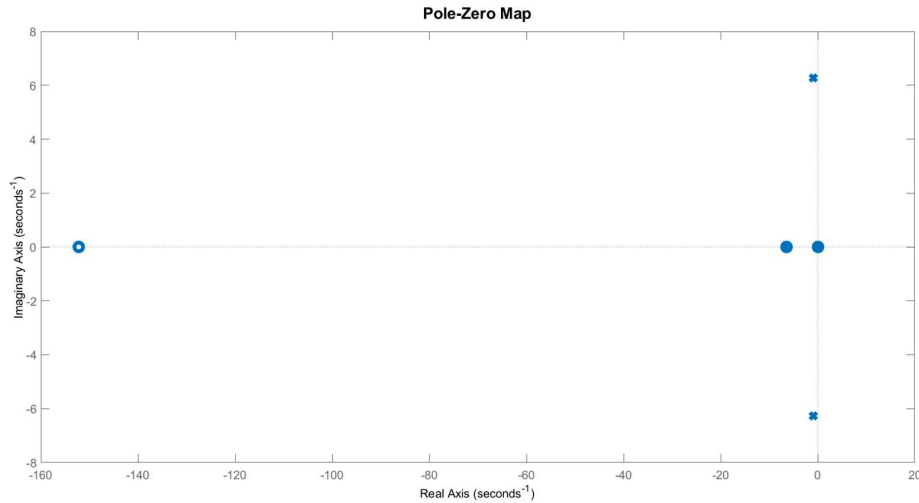


Figure 27. Pole-Zero Map of $\frac{\partial \beta}{\partial \text{Rudder}}$

$$\Rightarrow \frac{\partial p}{\partial \text{Rud}} = \frac{-0.45425 (s+6.081)(s^2 + 0.8982 + 2.994)}{(s+6.594)(s+0.05541)(s^2 + 1.707s + 39.95)}$$

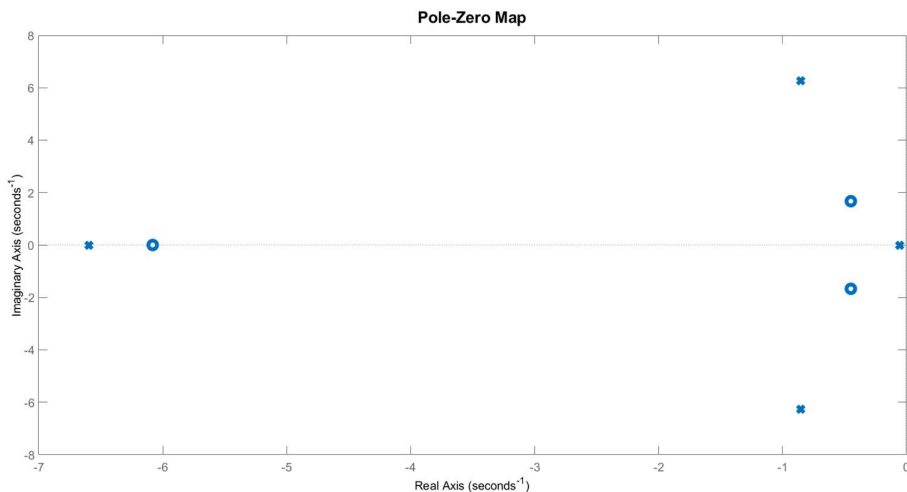


Figure 28. Pole-Zero Map of $\frac{\partial r}{\partial \text{Rudder}}$

5 FLIGHT CONTROLLER DESIGN

For the NASA-GTM aircraft, the control surface limits are provided in the Table 8. Controllers have been designed considering these limits, ensuring that the control signals do not exceed these limits, and anti-windup structures have been utilized for the integrator.

Table 8. Control surface limits

Elevator limits ($^{\circ}$)	[−30.0, 30.0]
Aileron limits ($^{\circ}$)	[−20, 20]
Rudder limits ($^{\circ}$)	[−30, 30]
Throttle limits (%)	[0, 100]
Stabilizer limits ($^{\circ}$)	[−12.0, 4.0]

Stabilizer is not used for this project.

5.1 Longitudinal Controller

A longitudinal controller, found in aircraft, is tasked with regulating the vehicle's longitudinal motion. This motion entails movement along the aircraft's longitudinal axis, an imaginary line extending from the front to the rear of the vehicle.

Longitudinal controller is primarily involved in managing pitch. Pitch refers to the aircraft's rotation about its lateral axis, causing the nose to ascend or descend. The longitudinal controller adeptly oversees this pitch motion, ensuring the maintenance of the desired attitude and stability throughout different flight phases, such as climbing, descending, or cruising.

The key components facilitating longitudinal control are the elevator surfaces, typically situated on the horizontal stabilizer of the aircraft's tail. These surfaces are adjusted by pilots or automated systems to govern the aircraft's pitch and uphold a predetermined flight trajectory. Longitudinal control plays a pivotal role in the overall stability and governance of an aircraft, ensuring a fitting response to pilot commands or automated control inputs.

5.1.1 Stability Augmentation, Pitch Damper (q-SAS)

Generally, incorporating pitch attitude feedback enhances the damping of the phugoid mode at the expense of the short period mode's damping.

The pitch damper, an important component of the longitudinal control system, utilizes the elevator to damp any pitch disturbances beyond the output of the aircraft's inherent longitudinal stability. This system is designed to enhance the longitudinal stability characteristics of an aircraft, particularly beneficial when the pitch is inadequately damped. The targeted stability derivatives, Cm_q and Cm_α , contribute to an increased damping ratio for the short period mode.

A fundamental pitch damper, serving as a part of the longitudinal control system, employs the elevator to damp disturbances in pitch beyond the output of open-loop longitudinal stability. This system plays a crucial role in strengthening the longitudinal stability characteristics of an aircraft.

The feedback of pitch - q (deg/s) obtained from the rate sensor model is added to the elevator command.

5.1.2 Inner Loop, Pitch Attitude Hold

Pitch Attitude Hold serves as a cruise/climb control function, commonly utilized during wing-level flight. Traditional pitch attitude control systems predominantly rely on the elevator as the control input. Controlling the flight path angle necessitates simultaneous management of airspeed.

Any deflection of the elevator or variation in throttle setting alters the pitch angle, impacting both the angle of attack and climb angle. In longitudinal control, where angle of attack and climb angle are coupled, a single input yields a singular output the pitch angle.

Pitch attitude proves to be a critical flight variable in both short and phugoid (long-period) modes. In the design of the pitch attitude hold system, an increase in controller gain shifts the short period mode roots toward the imaginary axis in root locus. This indicates that higher gain renders the aircraft longitudinally less stable dynamically. It's important to note that the controller doesn't maintain a constant climb angle due to variations in angle of attack over time, influenced by fuel burn and changing vehicle weight.

For the control law, integrating an integral term can eliminate steady-state error, and pitch attitude feedback significantly enhances phugoid damping.

Pitch attitude hold controller scheme is given in Figure 29.

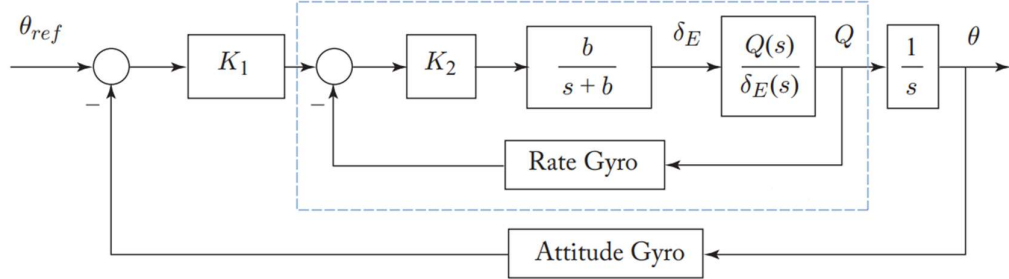


Figure 29. Pitch attitude hold controller block diagram

In NASA-GTM model this scheme is created as in Figure 30.

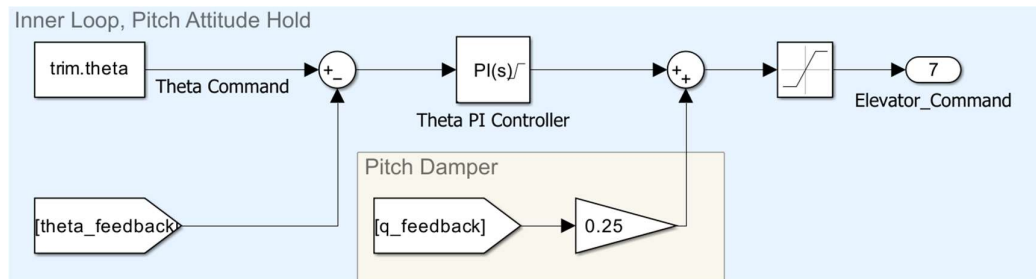


Figure 30. Pitch attitude hold controller design

- Initial theta command is the value of theta around the trim points. So, the nonlinear aircraft model firstly try to keep trimmed situation.
- Theta and q feedback are the modeled sensors outputs.
- When theta command is changed, error between feedback is considered via controller and necessity elevator value is commanded. The signal is summed with pitch damper value with a gain to increase longitudinal stability of the system.
- PI Controller includes initial integrator value so that trimmed elevator command will directly apply at the earlier of the simulation.
- Controller output is saturated between $[-30^\circ, 30^\circ]$ which are model elevator bounds in degrees. Saturation block is also added before the elevator command. Anti-windup is activated within the controller.

- Theta command and feedback units are degree, the unit of q is deg/s and elevator command unit is also degree.

Controller gains are given in Table 9.

Table 9. Pitch attitude hold controller gains

Proportional (P)	-1.3
Integral (I)	-0.5
q-SAS	0.25

5.1.3 Outer Loop, Altitude Hold

In the altitude hold mode, the aircraft's flight path angle, and consequently its altitude, are regulated using the elevator. Simultaneously, the airspeed or Mach number is managed through adjustments to the engine throttle. This mode requires a single feedback loop for altitude, which is measured by an altimeter, typically through GPS, a pitot tube, or radar altimeter.

The structure of an altitude control system closely resembles that of a rate of climb (or rate of descent) control system. The altitude hold autopilot is designed to maintain a specified altitude during specific flight phases, such as cruise. For the continuous maintenance of a specific cruise altitude, either the elevator or throttle can be employed. One approach involves maintaining constant throttle (engine thrust), allowing the elevator to decrease the angle of attack as the aircraft's weight diminishes. The longitudinal control system ensures that the aircraft holds a consistent altitude.

Altitude hold controller scheme is given in Figure 31.

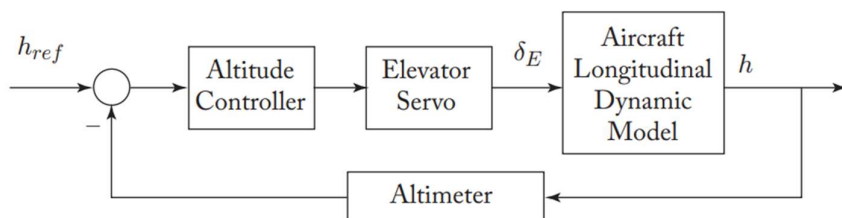


Figure 31. Altitude hold controller block diagram

In nonlinear model altitude hold scheme is created as in Figure 32.

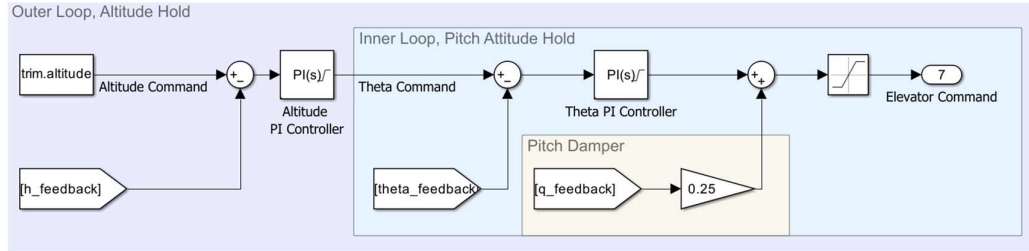


Figure 32. Altitude hold controller design

- Initial altitude command is the value of altitude around the trim points. So, the nonlinear aircraft model firstly try to keep trimmed situation.
- Altitude feedback is the modeled sensor output.
- When altitude command is changed, error between feedback is considered via controller and necessity theta value is commanded at the outer loop. Necessity elevator signal is created at the inner loop to achieve desired altitude.
- PI Controller includes initial integrator value so that trimmed theta command will directly apply at the earlier of the simulation.
- Controller output is saturated between $[-10^\circ, 10^\circ]$ to keep theta command between safe intervals. Anti-windup is activated within the controller.
- Altitude feedback unit is feet.

Altitude hold controller gains are given in Table 10.

Table 10. Altitude hold controller gains

Proportional (P)	0.3
Integral (I)	0.075

5.1.4 True Airspeed (TAS) Control

In the True Airspeed control mode, the aircraft is directed to maintain a constant velocity by autonomously adjusting the flight path angle and airspeed through the elevator and throttle. To initiate this mode, the aircraft is initially trimmed for straight and level flight, and the engine power is adjusted to achieve the desired velocity. Subsequently, the TAS controller mode of the flight control system is activated.

As the aircraft cruises, its weight decreases due to fuel consumption. If no pilot input is applied, there is a tendency for the speed and/or altitude to increase, resulting in a gradual climb. The control system detects this increase in speed and addresses it either by sending an up-elevator signal or by reducing the throttle. Throttle reduction causes the aircraft to decelerate, while the up-elevator signal induces a nose-down attitude, effectively counteracting the undesired climb. This corrective process ensures that the aircraft maintains the specified velocity during its flight.

True Airspeed controller scheme is given in Figure 33. In the scheme, M refers to Mach number. Instead of Mach number, True Airspeed is used in the project.

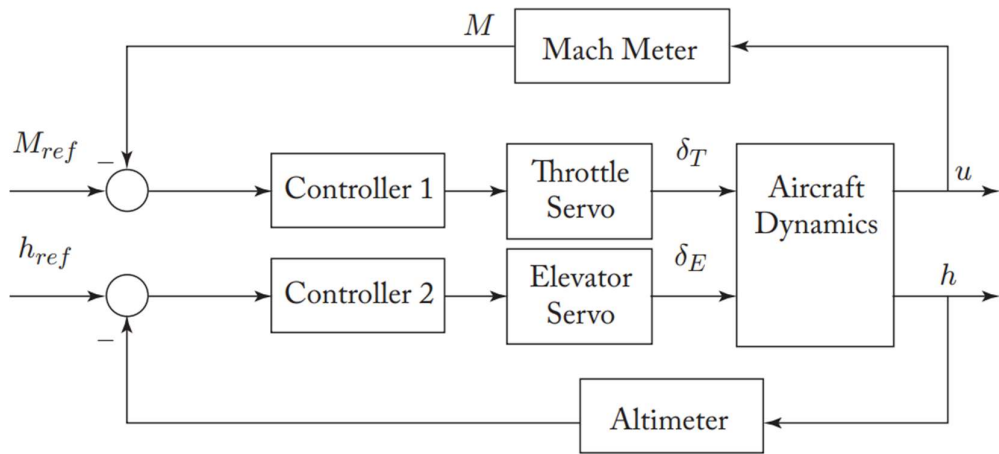


Figure 33. Velocity controller block diagram

TAS Controller scheme is created as in Figure 34.

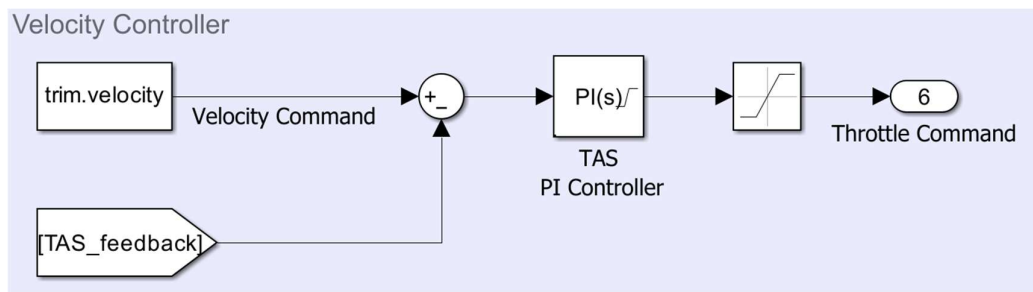


Figure 34. Velocity controller design

- Initial velocity command is the value of velocity around the trim points. So, the nonlinear aircraft model firstly try to keep trimmed velocity.
- TAS feedback is the modeled sensor output.

- When velocity command is changed, error between feedback is considered via controller and necessity throttle value is commanded. Throttle command can be between [%0, %100] theoretically but for “%0” throttle command the engine will shut down. Therefore, minimum limit needs to be greater than zero for real implementation.
- PI Controller includes initial integrator value so that trimmed throttle command will directly apply at the earlier of the simulation.
- Anti-windup is activated within the controller.
- TAS feedback unit is knots.

Controller gains of velocity are given in Table 11.

Table 11. TAS controller gains

Proportional (P)	4.5
Integral (I)	0.25

5.2 Lateral Controller

A lateral controller, in the context of aircraft or vehicle control systems, is responsible for managing lateral motion, which involves movement across the vehicle's lateral axis. The lateral axis is an imaginary line running from one side of the vehicle to the other.

In aviation, a lateral controller is primarily associated with controlling the roll motion of an aircraft. Roll refers to the rotation of the aircraft around its longitudinal axis, causing one wing to rise while the other descends. The lateral controller typically operates the ailerons, which are control surfaces on the wings that control roll by moving up or down.

The primary goal of a lateral controller is to maintain the desired bank angle and ensure the lateral stability of the aircraft during various phases of flight, such as turns or maneuvers. Automated systems or pilots use the lateral controller to input commands that adjust the ailerons and control the aircraft's roll motion.

In summary, a lateral controller is a crucial component of an aircraft's control system that focuses on managing lateral motion, particularly the roll motion around the longitudinal axis.

5.2.1 Stability Augmentation, Roll Damper (p-SAS)

Roll damper technique is enhancing directional stability, contributing to a more stable and steady flight.

Modern high-performance fighters, large transport aircraft, and many general aviation (GA) aircraft often encounter instability in lateral motions. These aircraft lack a natural tendency to return to their initial bank angles when disturbed. One effective solution to address this issue is the implementation of a Proportional-Integral (p-SAS) system.

The roll damper, a key component of lateral control systems, utilizes the aileron to dampen any disturbances in roll beyond the output of the aircraft's inherent lateral stability, if any. This roll control system is employed to improve the lateral stability characteristics of an aircraft. Its positive effects extend to the design of the wing, horizontal stabilizer, and vertical tail, particularly when dealing with lightly damped roll conditions.

The feedback of roll - p (deg/s) obtained from the rate sensor model is added to the aileron command.

5.2.2 Inner Loop, Wing Leveler

By definition, a wing-level autopilot maintains a zero-bank angle ($\phi = 0$) or holds a constant roll angle. Several factors can disrupt a state of wings-level, including structural asymmetry, engine torque, atmospheric turbulence, and fuel slosh. In gusty conditions, one side of the wing (left or right) tends to drop, and even in smooth air, one side of the wing may eventually dip. Without autopilot intervention, the aircraft naturally tends to roll. This indicates that air vehicles do not inherently possess roll stability, although they may exhibit lateral stability.

To achieve the goal of maintaining wings-level flight, the primary control surface employed is the aileron (δ_A). The aileron is crucial in counteracting and controlling the rolling tendencies induced by external forces and disturbances, ensuring the aircraft remains in a desired bank angle or roll attitude.

Wing Leveler controller scheme is given in Figure 35.

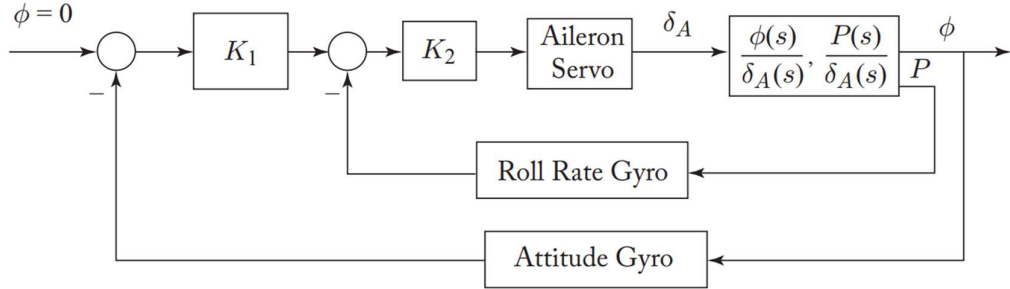


Figure 35. Wing leveler controller block diagram

In nonlinear model the controller scheme is created as in Figure 36.

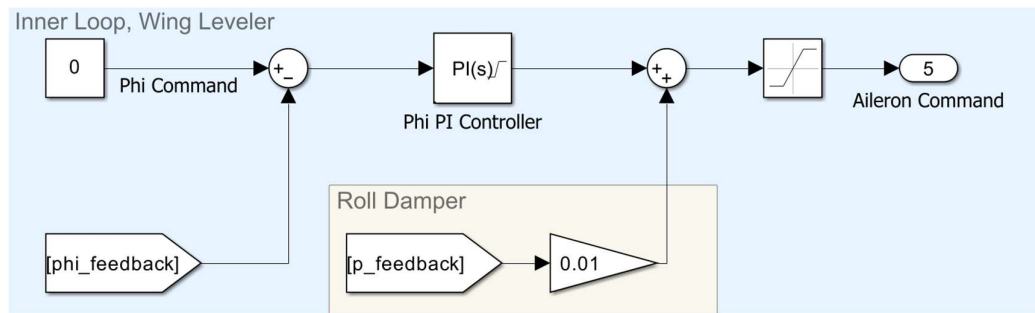


Figure 36. Wing leveler controller design

- Initial phi angle command is zero. So, the nonlinear aircraft model tries to not roll.
- Roll angle phi and roll rate p feedbacks are the modeled sensors outputs.
- When phi command is changed, error between feedback is considered via controller and necessity aileron value is commanded. The signal is summed with roll damper value with a gain to increase lateral stability of the system.
- PI Controller includes initial integrator value so that trimmed aileron command will directly apply at the earlier of the simulation.
- Controller output is saturated between $[-20^\circ, 20^\circ]$ to keep aileron command between safe intervals. Anti-windup is activated within the controller.
- Phi command and feedback units are degree, the unit of p is deg/s and aileron command unit are also degree.

Controller gains of wing leveler are given in Table 12.

Table 12. Wing leveler controller gains

Proportional (P)	-0.1
Integral (I)	-0.012

5.2.3 Outer Loop, Heading Angle Hold

The heading angle, denoted by the symbol Ψ , is the angle between the longitudinal axis of an aircraft and a reference direction, typically measured in the horizontal plane. This reference direction is often defined as true North or magnetic North. The heading angle provides information about the direction in which the nose of the aircraft is pointing.

The heading angle is distinct from the course angle, which represents the actual direction in which the aircraft is moving through the air. While the heading angle indicates where the aircraft is pointing, the course angle considers the effects of wind and other factors on the aircraft's track over the ground.

A heading angle hold controller is a component of an aircraft's autopilot system designed to maintain a specific heading angle. The autopilot utilizes various sensors and feedback mechanisms to continuously adjust the aircraft's control surfaces, typically the ailerons, to ensure that it stays on a predetermined heading.

Heading angle hold controller scheme is given in Figure 37.

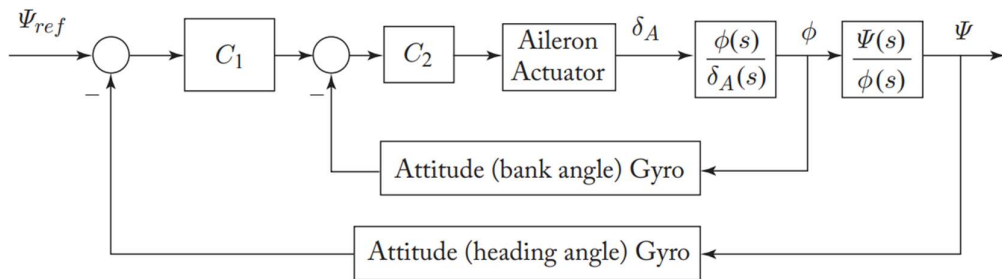


Figure 37. Heading angle controller block diagram

In nonlinear model controller scheme is created as in Figure 38.

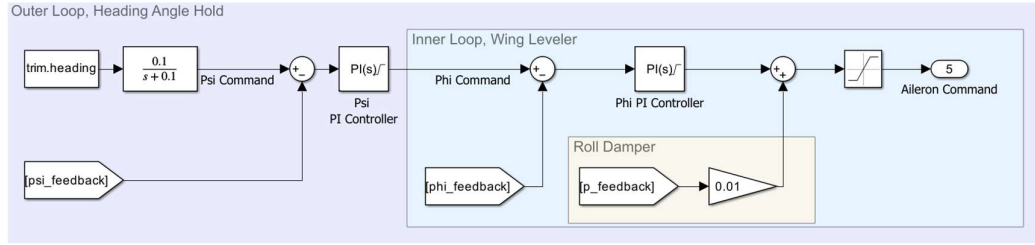


Figure 38. Heading angle controller design

- Initial heading angle-psi command is the value of the heading angle around the trim points. So, the nonlinear aircraft model starts from this heading angle and keeps it.
- Psi feedback is the modeled sensors output.
- Heading angle-psi command is filtered. Therefore, Psi commands will not be change from one angle to commanded angle directly. It will take some time for signal to achieve command. Time constant of the filter is $\tau = 10$. The difference between direct signal and filtered signal is given in Figure 39.

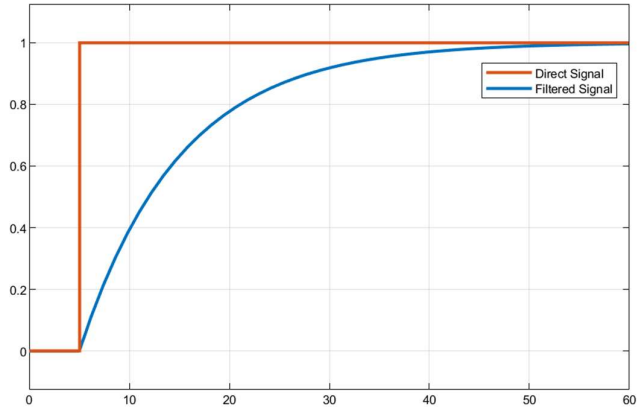


Figure 39. Direct and filtered signal comparison

- When heading command is changed, error between feedback is considered via controller and necessity phi signal is commanded at the outer of the loop. Necessity aileron signal is commanded at the inner loop to achieve desired attitude.
- PI Controller includes initial integrator value so that trimmed phi command will directly apply at the earlier of the simulation.

- Controller output is saturated between $[-10^\circ, 10^\circ]$ to keep roll angle-phi command between safe intervals. Anti-windup is activated within the controller.
- Heading angle-psi feedback unit is degree.

Heading angle controller gains are given in Table 13.

Table 13. Heading angle controller gains

Proportional (P)	0.5
Integral (I)	0.01

The heading angle controller is a controller that ensures the aircraft maintains the desired heading angle, as given by Figure 40. This controller is used to ensure that the aircraft aligns with the same orientation as the runway before landing.

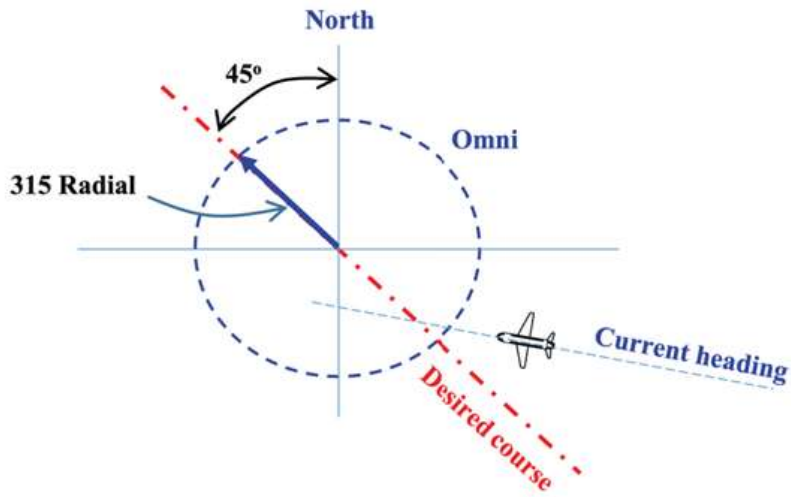


Figure 40. Heading angle alignment

5.2.4 Sideslip Angle Control

Sideslip angle control, specifically linking the sideslip angle (β) to the rudder, is a function within an aircraft's control system that manages the aircraft's lateral motion. The sideslip angle is the angle between the aircraft's longitudinal axis and the direction of its actual flight path. This angle is a result of the aircraft's sideslip motion, which can occur due to factors such as crosswinds or yawing moments.

In sideslip angle control, the rudder is a primary control surface used to regulate and control the sideslip angle. The sideslip angle can have implications for the aircraft's stability, handling, and aerodynamic performance.

In crosswind conditions or during certain flight maneuvers, the sideslip angle control ensures that the aircraft remains stable and responsive to the pilot's or autopilot's inputs. Proper sideslip angle management is crucial for safe and efficient flight, particularly during takeoff, landing, and other critical phases of operation.

Sideslip angle is given in Figure 41.

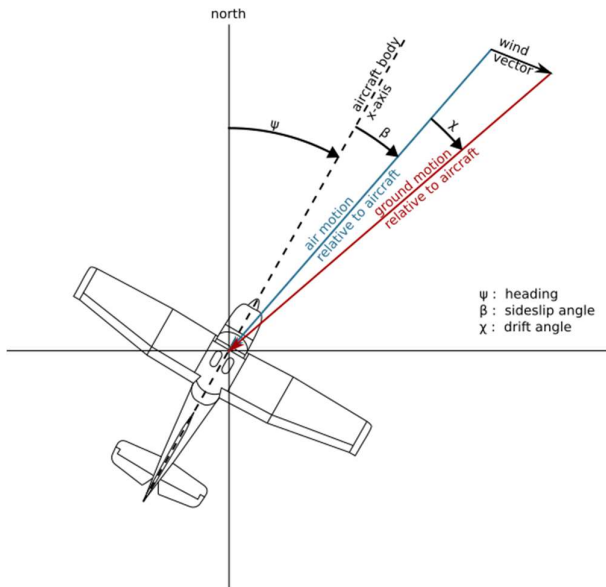


Figure 41. Sideslip - β angle representation

In nonlinear model sideslip angle controller is created as in Figure 42.

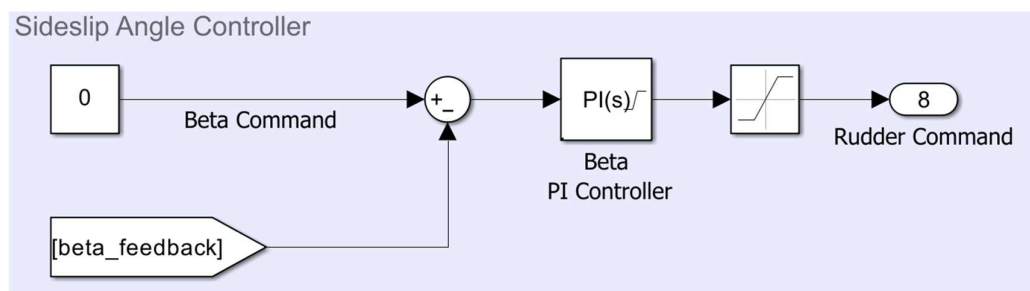


Figure 42. Sideslip angle controller design

- Initial beta command is zero means that no side wind is assumed, aircraft flights with zero sideslip angle.

- Beta feedback is the modeled sensors output.
- When beta command is changed, error between feedback is considered via controller and necessity rudder value is commanded.
- Controller output is saturated between $[-30^\circ, 30^\circ]$ to keep rudder command between safe intervals. Anti-windup is activated within the controller.
- Beta feedback unit is degree.

Controller gains of sideslip angle are given in Table 14.

Table 14. Sideslip angle controller gains

Proportional (P)	1
Integral (I)	0.1

6 SIMULATION AND RESULTS

The simulation environment is MATLAB/SIMULINK. The aircrafts model and controllers are implemented in the SIMULINK environment. Scripts in the MATLAB environment are used for open systems linear and nonlinear comparisons and analyses. To enhance the observation of aircraft behavior, the FlightGear simulator program has been integrated into the project, allowing for visual analysis of model behaviors. The aircraft used for visualization purposes in the FlightGear environment is the Boeing 777-300, as shown in Figure 43.

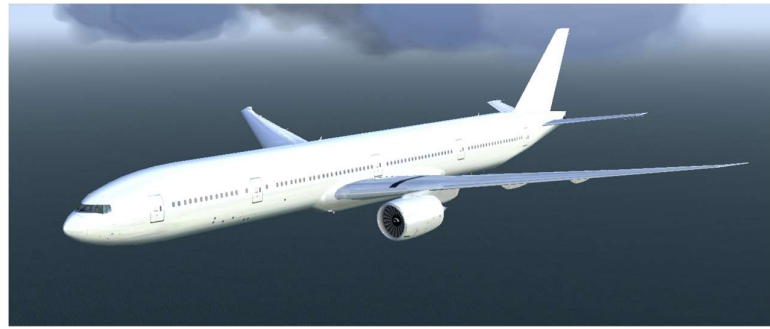


Figure 43. Boeing 777-300 in FlightGear simulator

6.1 Base Leg

Simulation begins with the aircraft in the Base Leg phase. The aircraft is initially at the altitude of 500 feet, and its speed is 75 knots. The aircraft is maintaining straight and level flight at this altitude and speed, without performing any turning maneuvers. The behavior of the aircraft at this stage is depicted in the Figure 44.

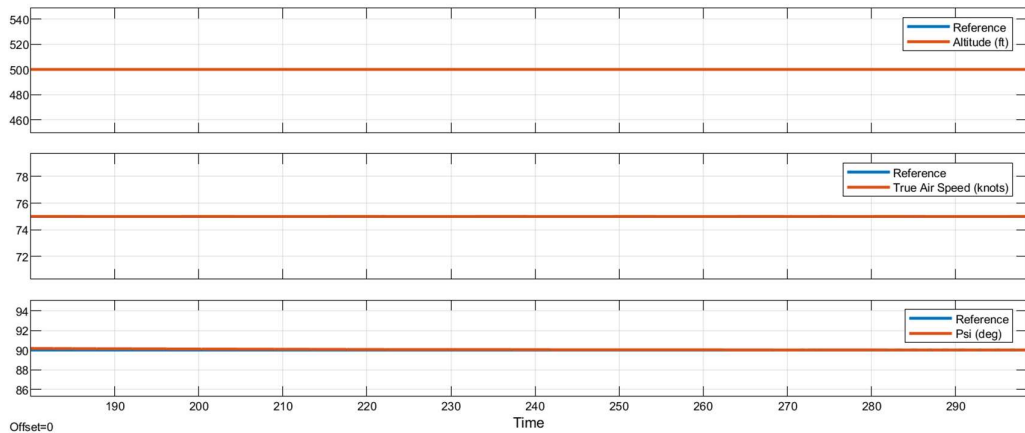


Figure 44. Altitude, TAS and heading angle graphics

6.1.1 Heading Angle Arrangement

In the simulation environment, the initial heading angle (Ψ) of the aircraft is 90 degrees. Assuming that the runway heading is at -90 degrees, so the aircraft is commanded to make two 90-degree turns, ensuring that it aligns its heading angle with the runway. Heading angle changes are achieved with the lateral controller as mentioned in section 5.2. During the roll maneuver, altitude and speed performances are given in Figure 45, heading angle and roll angle changes are given in Figure 46.

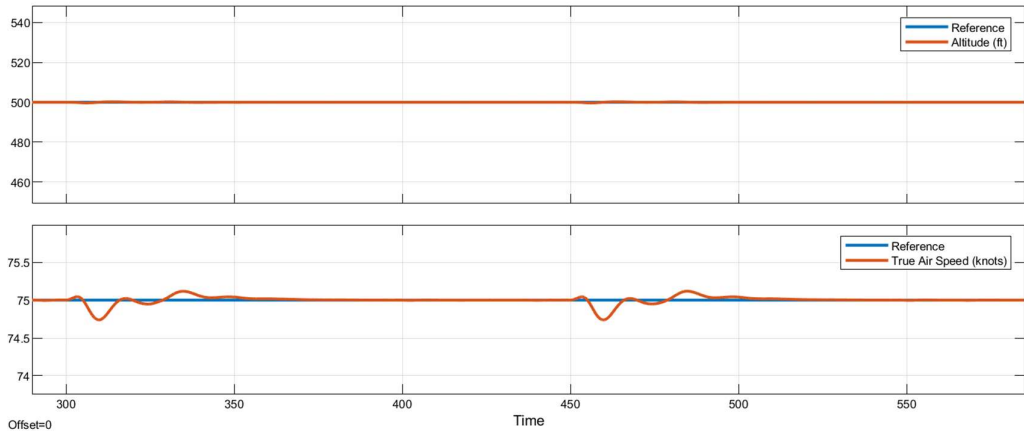


Figure 45. Altitude and TAS graphics during roll maneuver

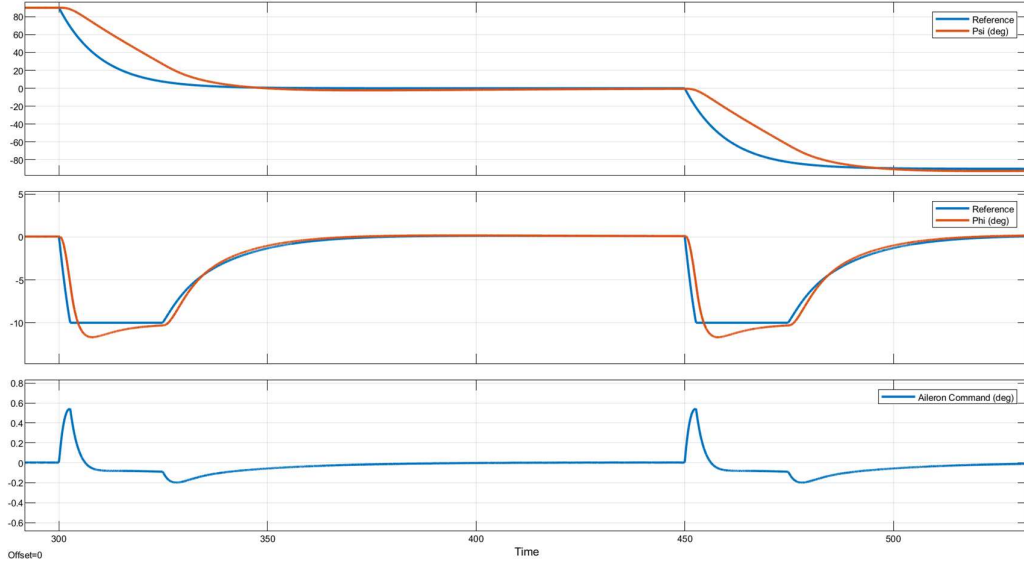


Figure 46. Lateral controller graphics during roll maneuver

During the heading angle arrangement Sideslip controller tries to keep beta angle as zero means no rudder command. This situation is given in Figure 47.

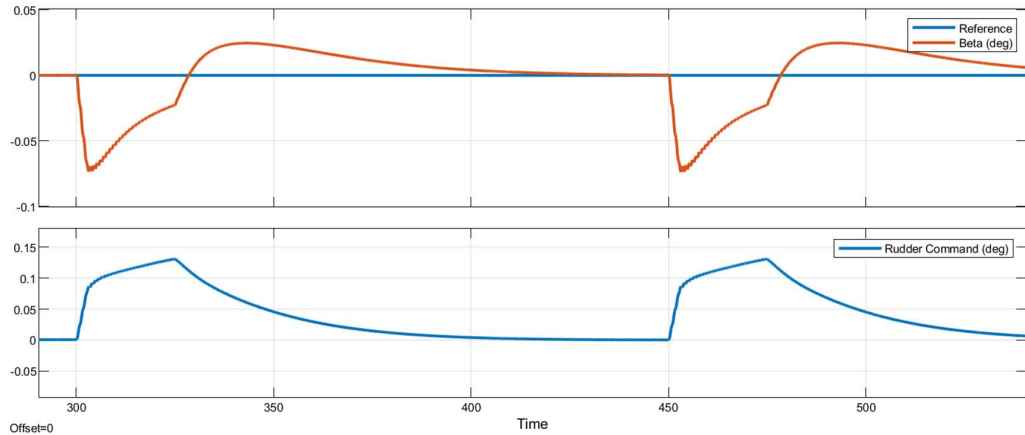


Figure 47. Sideslip angle controller graphic during roll maneuver

6.1.2 Speed Adjustment

To facilitate a smoother landing for the aircraft, a true airspeed (TAS) controller has been commanded to set the speed value to 60 knots before gliding. The behavior of the speed controller during this transition is depicted in Figure 48.

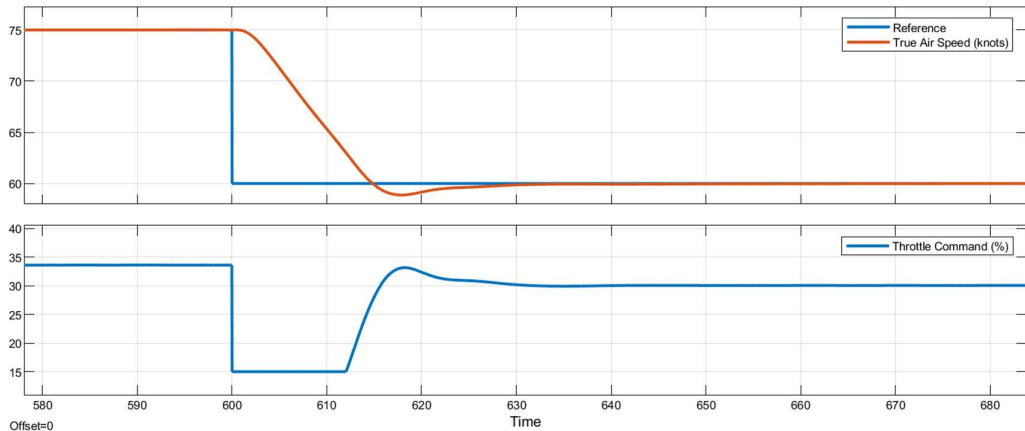


Figure 48. Velocity controller graphics during speed adjustment

The aircraft has reduced thrust to achieve the required speed value. During this time, the altitude controller is still commanding a constant altitude. To maintain a constant altitude, the aircraft has adjusted the pitch angle (θ) accordingly. This situation is depicted as given by Figure 49.

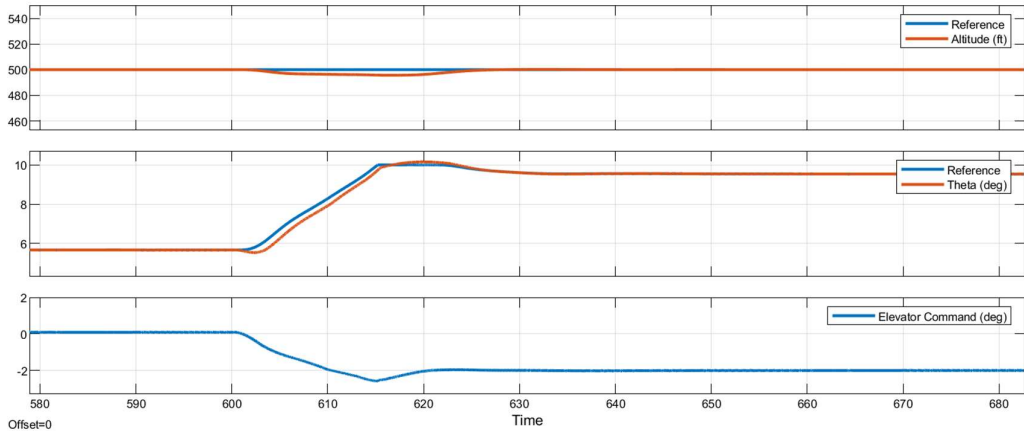


Figure 49. Longitudinal controller graphics during speed adjustment

6.1.3 Flaps Extension

The flaps are extended 15° before the gliding phase. This serves several important purposes as follows.

- *Increased Lift*: Flaps, when extended, increase the wing's surface area, and change its shape. This increases the lift generated by the wings at a given airspeed, allowing the aircraft to maintain lift at lower speeds.
- *Reduced Stall Speed*: The increased lift provided by flaps allows the aircraft to maintain controlled flight at lower speeds, reducing the stall speed. This is particularly important during the approach and landing when the aircraft needs to descend at a controlled rate.
- *Steep Approach Capability*: Flaps enable the aircraft to execute a steeper approach angle without increasing the airspeed excessively. This is beneficial for landing on shorter runways or in confined spaces.
- *Enhanced Control Authority*: Flaps provide additional control authority, especially at low speeds. This increased control allows for better handling during the critical phases of landing, such as flare and touchdown.
- *Reduced Landing Distance*: The increased lift and drag from extended flaps result in a slower approach and landing speed, contributing to a shorter landing distance. This is particularly advantageous when landing on shorter runways.

Flaps are extended when $Time = 700$. The behavior of the speed controller during the extension is depicted in Figure 50.

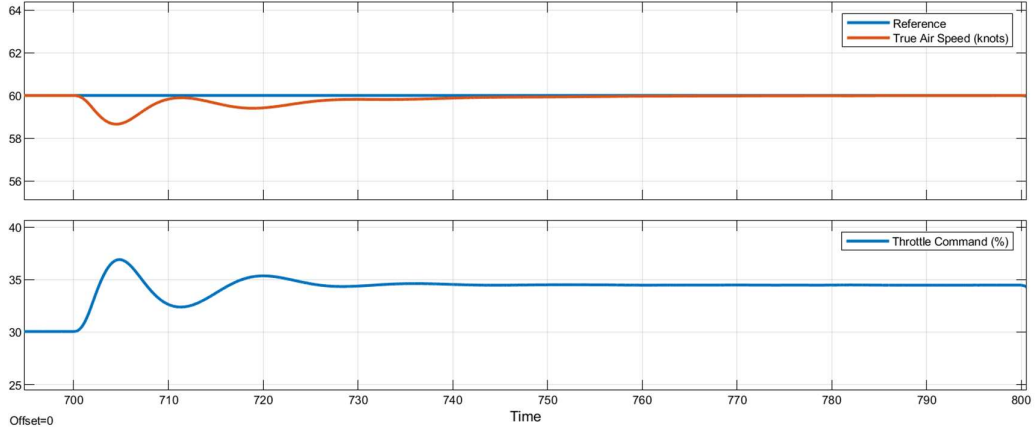


Figure 50. Velocity controller graphics during flaps extension

Theta angle is also changed after the flaps extension. The reason is same as mentioned in the speed adjustment.

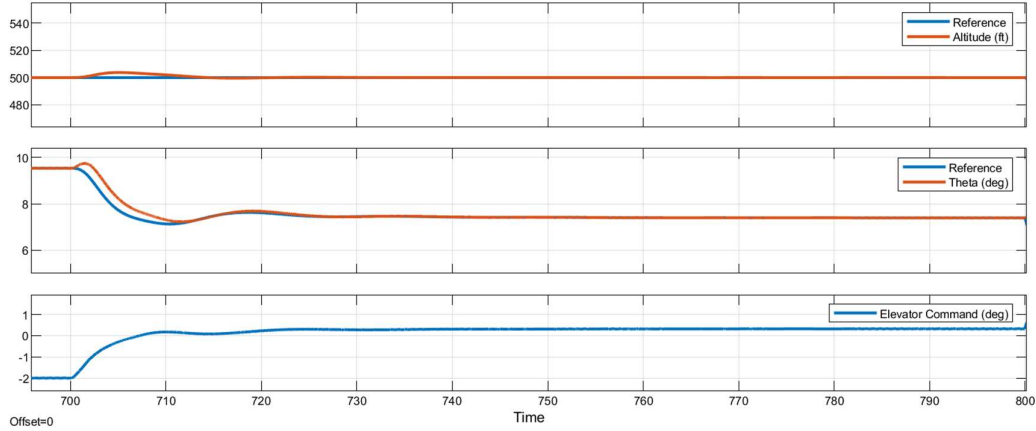


Figure 51. Longitudinal controller graphics during flaps extension

6.2 Glide Phase

In the case of glide phase, recommended approach glide slope ranges from 2.5 to 3.5. For this reason, gamma angle is chosen as $\gamma = 2.5$.

The altitude command initiates at 500 feet and is linearly commanded to decrease up to the starting altitude of the flare phase, which is 50 feet.

The altitude command is computed as follows.

$$h(t + 1) = h(t) - V_{TAS} * \sin(\gamma = 2.5^\circ) * (knots - to - feet/second)$$

$$knots - to - feet/second = 1.68781$$

During the landing True Airspeed is also decreased linearly from 60 knots to 55 knots.

Aircraft longitudinal behavior is given in Figure 52.

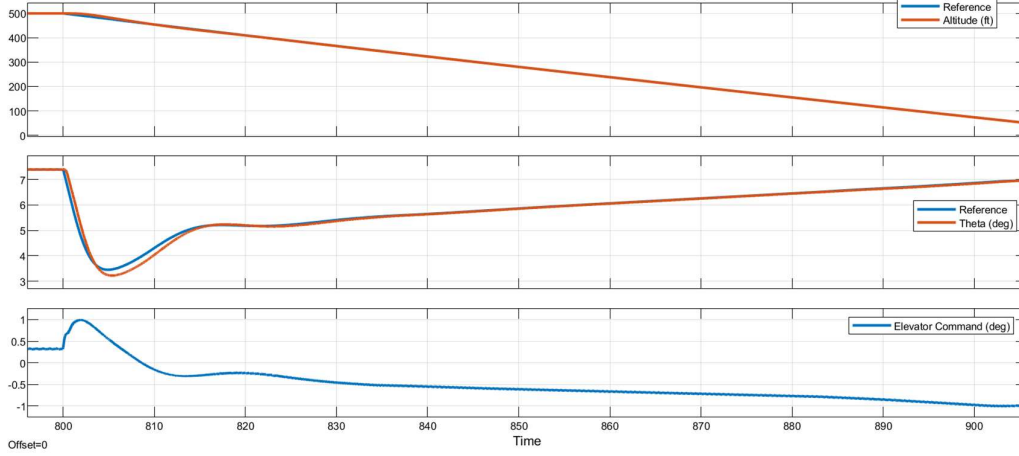


Figure 52. Longitudinal controller graphics at glide phase

When the altitude command begins to decrease, the aircraft pitches downward, reducing the theta angle, and as a result, the speed increases slightly. Later, the desired speed command is adjusted with the controller as in Figure 53.

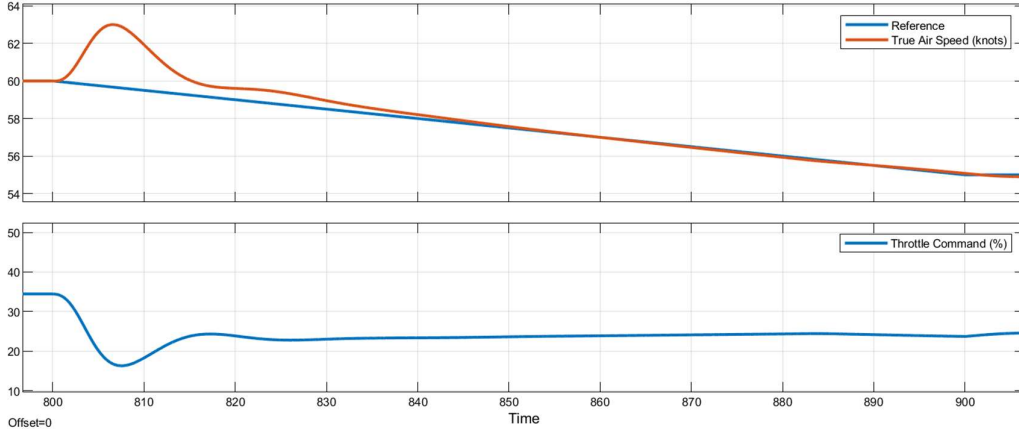


Figure 53. Velocity controller graphics at glide phase

Gamma angle γ and vertical speeds are given in Figure 54. As mentioned, we are aiming to glide with a gamma angle of $\gamma = 2.5^\circ$ degree.

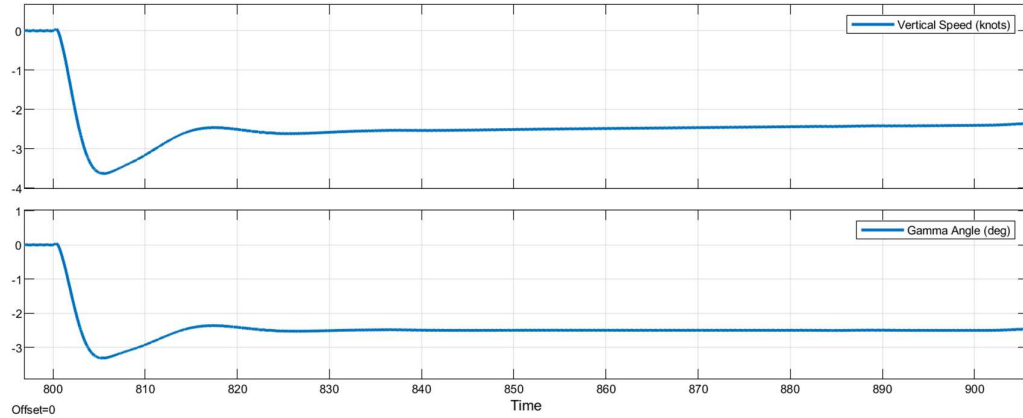


Figure 54. Vertical speed and gamma angle graphics at glide phase

6.3 Flare Phase

Flare phase is started at 50 feet above the ground and the aircraft try to keep the air speed as 55 knots. An automatic flare control directs the aircraft to follow an exponential path from the beginning of the flare until touchdown like in Figure 55. Altitude command that represents the exponential curve with a negative slope is as follows.

$$h(t) = h_0 e^{-\frac{t}{\tau}}; \tau = 10$$

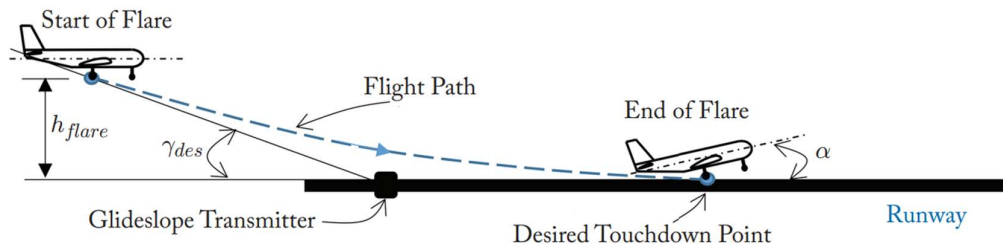


Figure 55. Desired exponential flare path

Aircraft longitudinal behavior is given in Figure 56.

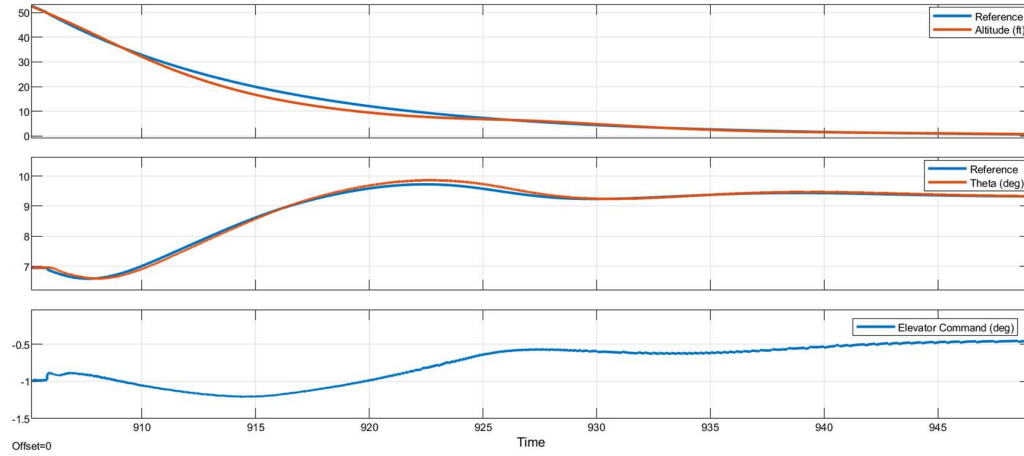


Figure 56. Longitudinal controller graphics at flare

During the flare, which is the final approach phase, the nose of the aircraft is raised (pitching up) to reduce the descent rate and establish the correct attitude for a smooth touchdown. Therefore, airspeed decreased a little as seen in Figure 57.

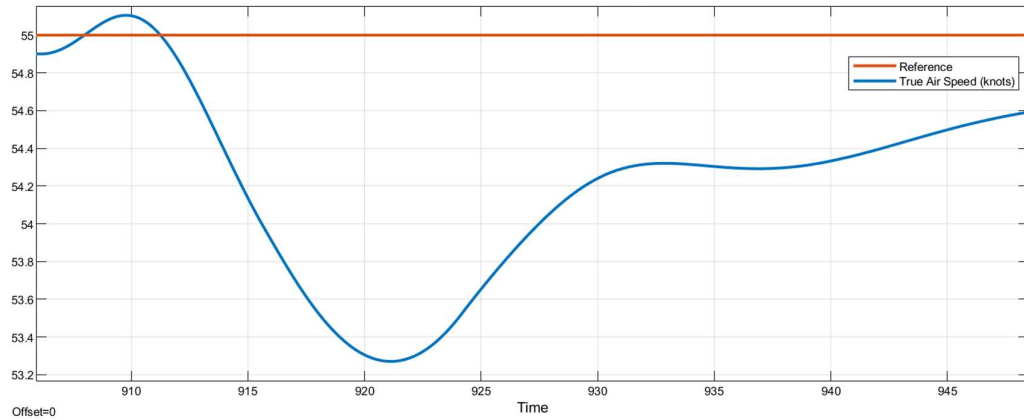


Figure 57. Velocity behavior at flare

As seen from the above figure minimum air speed value during the flare is 53.5 knots which is above the stall speed. Stall speeds according to flaps position for the NASA-GTM aircraft are given in Table 15.

Table 15. Stall speeds according to flaps position

Flaps Position	Stall Speed
0°	51.6
15°	46.1
30°	40.6

Flaps were extended 15° in the Base Leg phase.

Gamma angle γ and vertical speeds for this phase is given in Figure 58.

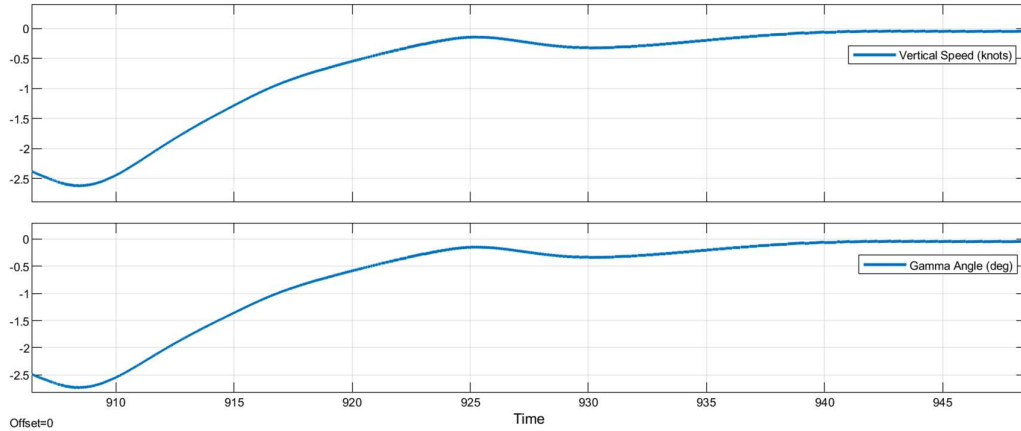


Figure 58. Vertical speed and gamma angle graphics at flare

6.4 Touchdown

If an aircraft touches down with a descent rate ranging from 0 to 1.5 knots, it is classified as a soft landing and is strongly recommended. However, if the descent rate at touchdown falls within the range of 1.5 to 7 knots, it is categorized as a hard landing. A descent rate within this range is considered unacceptable from a flying qualities perspective (exceeding vertical speed limits). Upon contact of the main landing gear with the runway, prompt de-rotation should take place.

As seen in Figure 58, touches down descent rate is between 0 and 0.5 knots. This means that, safe and soft landing is achieved.

The objective of this project was to perform a landing based on the aircraft's center of gravity (CG). Ground effects and landing gear models are not considered for this project.

REFERENCES

- 1 *Chester H. Wolowicz, J. S. (1979, August 1). NTRS - NASA Technical Reports Server. Retrieved December 3, 2023, from <https://ntrs.nasa.gov/citations/19790022005>*
- 2 *Cunningham, K., Cox, D. E., Murri, D. G., and Riddick, S. E., "A Piloted Evaluation of Damage Accommodating Flight Control Using a Remotely Piloted Vehicle," AIAA-2011-6451, AIAA Guidance, Navigation, and Control Conference and Exhibit, Portland Oregon, August 2011."*
- 3 *EA, Ahmed & Hafez, Ashraf & Ouda, A. & Ahmed, Hossam & Abd-Elkader, Hala. (2015). Design of Longitudinal Motion Controller of a Small Unmanned Aerial Vehicle. ijisa. 7. 37-47. 10.5815/ijisa.2015.10.05.*
- 4 *EA, Ahmed. (2015). Design of a Lateral Motion Controller for a Small Unmanned Aerial Vehicle (SUAU). 10.13140/RG.2.1.3407.9446.*
- 5 *Etkin B. (1972). Dynamics of atmospheric flight. Wiley.*
- 6 *Federal Aviation Administration. (2011). Airplane flying handbook (FAA-H-8083-3A). Skyhorse Publishing Inc..*
- 7 *Ha, C. K., & Ahn, S. W. (2003). Automatic Landing in Adaptive Gain Scheduled PID Control Law, 2345-2348.*
- 8 *Jordan, T., Langford, W., & Hill, J. (2005, August). Airborne subscale transport aircraft research testbed-aircraft model development. In AIAA Guidance, Navigation, and Control Conference and Exhibit (p. 6432).*
- 9 *Jordan, T., Langford, W., Belcastro, C., Foster, J., Shah, G., Howland, G., & Kidd, R. (2004, January). Development of a dynamically scaled generic transport model testbed for flight research experiments. In AUVSI's Unmanned Systems North America 2004 Symposium and Exhibition.*
- 10 *Le Roux, C. T. (2016). Autonomous landing of a fixed-wing unmanned aerial vehicle onto a moving platform (Doctoral dissertation, Stellenbosch: Stellenbosch University).*
- 11 *Lelardeux, C. P. (2017). Real-time Virtual Collaborative Environment Designed for Risk Management Training: Communication and Decision Making (Doctoral dissertation, Université Paul Sabatier (Toulouse 3)).*
- 12 *Lu, K., & Liu, C. (2019). A L 1 Adaptive Control Scheme for UAV Carrier Landing Using Nonlinear Dynamic Inversion. international journal of aerospace engineering, 2019.*
- 13 *McLean, D. (2003). Automatic flight control systems. Measurement and Control, 36(6), 270–310. <https://doi.org/10.1177/002029400303600602>*
- 14 *Nho, K., & Agarwal, R. K. (2000). Automatic landing system design using fuzzy logic. Journal of Guidance, Control, and Dynamics, 23(2), 298-304.*

- 15 Norouzi, R. (2018, July). *Reconfiguring NASA Generic Transport Model for Normal Flight Envelope Simulation and Analysis*. In *2018 9th International Conference on Mechanical and Aerospace Engineering (ICMAE)* (pp. 45-52). IEEE.
- 16 Nugroho, L. (2014, October). *Comparison of classical and modern landing control system for a small unmanned aerial vehicle*. In *2014 International Conference on Computer, Control, Informatics and Its Applications (IC3INA)* (pp. 187-192). IEEE.
- 17 Pashilkar, A. A., Sundararajan, N., & Saratchandran, P. (2006). *A fault-tolerant neural aided controller for aircraft auto-landing*. *Aerospace Science and Technology*, 10(1), 49-61.
- 18 Rao, D. V., & Go, T. H. (2014). *Automatic landing system design using sliding mode control*. *Aerospace Science and Technology*, 32(1), 180-187.
- 19 Sadraey, M. (2020). *Automatic flight control systems*. Morgan & Claypool Publishers.
- 20 Sonneveldt, L. (2010). *Adaptive Backstepping Flight Control for Modern Fighter Aircraft*. Delft, The Netherlands: Ph.D. Thesis.
- 21 Stevens, B. L., Lewis, F. L., & Johnson, E. N. (2015). *Aircraft control and simulation: dynamics, controls design, and autonomous systems*. John Wiley & Sons.
- 22 Yavrucuk, I. ve Kargin, V. (2008). *Autolanding Strategies for a Fixed Wing UAV in Adverse Atmospheric Conditions*, AIAA Guidance, Navigation and Control Conference and Exhibit, s.6963.

APPENDIX

This project is available as open source on GitHub. The project is not finalized with this thesis; instead, it is designed as an ongoing open-source project that will be continuously developed.

The NASA-GTM aircraft model is currently hosted on GitHub. The repository is as follows.

➤ ***The Generic Transport Model***

https://github.com/nasa/GTM_DesignSim

Project is based on the given aircraft model, and an integrated working environment has been established using the Git system. This allows for more organized tracking of the project, enhances accessibility, and ensures that all files are recorded through Git instead of progressing through file transfers.

The final version of the project can be accessed via the following GitHub link. This provides an opportunity to examine the development stages of the project, transitions between versions, and version descriptions.

➤ ***Controller Design***

https://github.com/FurkanCiftlikci/GTM_DesignSim_Controller_Design

ÖZGEÇMİŞ

Ad-Soyad : Furkan Çiftlikci
Doğum Tarihi ve Yeri : 30/10/2000 - Kayseri
E-posta : ciftlikci21@itu.edu.tr



ÖĞRENİM DURUMU:

- **Lisans** : 2024, İstanbul Teknik Üniversitesi, Elektrik ve Elektronik Fakültesi, Kontrol ve Otomasyon Mühendisliği (%100 İng.)
- **Lisans** : 2021, Yıldız Teknik Üniversitesi, Elektrik ve Elektronik Fakültesi, Kontrol ve Otomasyon Mühendisliği (%100 İng.)

MESLEKİ DENEYİM VE ÖDÜLLER:

- 2022 yılında TEKNOFEST, TÜBİTAK Uluslararası Serbest Görev İha Yarışması Kategorisi Türkiye Üçüncülüğü ödülü aldı.
- 2022 Ağustos-Eylül aylarında BAYKAR TEKNOLOJİ firmasında stajyerlik yaptı.
- 2023 Mart'tan günümüze BAYKAR TEKNOLOJİ firmasında Kontrol ve Otomasyon Mühendisi olarak çalışmaktadır.

ÖZGEÇMİŞ

Ad-Soyad : Ebubekir Denizhan
Doğum Tarihi ve Yeri : 02/12/2000 - İstanbul
E-posta : denizhan18@itu.edu.tr



ÖĞRENİM DURUMU:

- **Lisans** : 2024, İstanbul Teknik Üniversitesi, Elektrik ve Elektronik Fakültesi, Kontrol ve Otomasyon Mühendisliği (%100 İng.)

MESLEKİ DENEYİM VE ÖDÜLLER:

- 2022 Haziran-Eylül aylarında TIMESOFT firmasında stajyerlik yaptı.
- 2023 Ocak-Temmuz aylarında TIMESOF firmasında yarı zamanlı web developer olarak çalıştı.
- 2023 Temmuz-Kasım aylarında BAYKAR TEKNOLOJİ firmasında stajyerlik yaptı.
- 2023 Aralık'tan günümüze BAYKAR TEKNOLOJİ firmasında Kontrol ve Otomasyon Mühendisi olarak çalışmaktadır.

ÖZGEÇMİŞ



Ad-Soyad : Agah Enes Soyalp
Doğum Tarihi ve Yeri : 24/02/2001 - Ankara
E-posta : soyalp19@itu.edu.tr

ÖĞRENİM DURUMU:

- Lisans** : 2024, İstanbul Teknik Üniversitesi, Elektrik ve Elektronik Fakültesi, Kontrol ve Otomasyon Mühendisliği (%100 İng.)

MESLEKİ DENEYİM VE ÖDÜLLER:

- 2020 yılında TEKNOFEST Roket Yarışması Alçak İrtifa Kategorisi Türkiye Üçüncülüğü ödülü aldı.
- 2021 yılında TÜBİTAK Serbest Görev İHA Yarışması Türkiye İkinciliği ödülü aldı.
- 2021 yılında TEKNOFEST Savaşan İHA Yarışması Sabit Kanat Kategorisi Türkiye Üçüncülüğü ödülü aldı.
- 2021 yılında TEKNOFEST Roket Yarışması Yüksek İrtifa Kategorisi Türkiye İkinciliği ödülü aldı.
- 2021 yılında TEKNOFEST Roket Yarışması Yüksek İrtifa Kategorisi En Bilimsel Faydalı Yük Özel Ödülü'nü aldı.
- 2021 Ağustos ayında Turksat Uydu'da stajyerlik yaptı.
- 2022 Ağustos ayında Roketsan Ankara'da stajyerlik yaptı.
- 2023 Mart'tan günümüze CEZERİ YZR firmasında yarı zamanlı Kontrol ve Otomasyon Mühendisi olarak çalışmaktadır.